AEROSPACE REPORT NO.
ATR-76(7475)-1

Analysis of Pogo on the Space Shuttle: Accumulator Design Guidelines and Planar Multiengine Model Development

Prepared by M. H. LOCK and S. RUBIN
Vehicle Engineering Division

September 1976

Prepared for

NATIONAL AERONAUTICS AND SPACE ADMINISTRATION
LYNDON B. JOHNSON SPACE CENTER
Houston, Texas 77058

Contract No. NAS9-14142
DRL T-1025
Line Item No. MA183TA

Engineering Science Operations
THE AEROSPACE CORPORATION

NAS9-14142
DRL T-1025
Line Item No.
MA183TA

ANALYSIS OF POGO ON THE SPACE SHUTTLE: ACCUMULATOR DESIGN GUIDELINES AND PLANAR MULTIENGINE MODEL DEVELOPMENT

13 September 1976

Prepared For

National Aeronautics and Space Administration
Lyndon B. Johnson Space Center
Houston, Texas 77058

Prepared By

M. H. Lock
S. Rubin

The Aerospace Corporation
El Segundo, California

FOREWORD

This report describes the results of pogo stability investigations undertaken at The Aerospace Corporation during the period June 1974 to October 1975. The work was performed under NASA contract NAS9-14142; the NASA (JSC) Technical Monitor was Dr. H. Doiron. The authors would like to acknowledge the work of Raymond E. Orth in programming the stability equations employed in the study and the constructive comments of Dr. Doiron during the course of the investigation.

ABSTRACT

This report presents the results of a study concerned with the prevention of pogo instability on the Space Shuttle. The study dealt with the main engine propulsion system and comprised two distinct efforts:

1. The development of design guidelines for a helium-charged accumulator based upon analyses undertaken with an equivalent single-engine stability model of the coupled Shuttle structural/propulsion system.

2. The development of a refined multiengine pitch plane stability model and the generation of initial stability results with this latter model.

The design guidelines were generated to support the selection of the baseline accumulator configuration for the Space Shuttle. They were based upon the elimination of the instabilities that had been predicted for the Shuttle system (in the absence of accumulators) using the single-engine model. The multiengine pitch plane stability model was subsequently developed to enable a more refined analysis of the pogo problem. The results obtained with this refined model, in the absence of accumulators, indicated a generally stable system. However, it was found that reasonable adjustment of the axial motion of the feedline aft support on the external tank could induce instability of the system. This instability was eliminated by the addition of high-pressure oxidizer turbopump (HPOTP) inlet accumulators to the system. The results obtained with the refined model did not suggest a need to alter the design guidelines that had been obtained previously.

The analyses with the multiengine model also treated the question of the use of a phase margin in the system stability requirements. The results in this case indicated that use of a phase margin in the manner given in the NASA Space Vehicle Design Criteria (Ref. 1) is not appropriate.

CONTENTS

TABLES

FIGURES

FIGURES (Continued)

FIGURES (Concluded)

NOMENCLATURE

Units: M (mass), F (force), L (length), T (time)

C	compliance, $[F^{-1}L^{5}]$
G_e	structural gain for engine motion, $\phi^2(e)/M$, $[M^{-1}]$
L	inertance, $[FL^{-5}T^{2}$ or $ML^{-4}]$
$n+1$	pump dynamic gain, [-]
M	mass, [M]
P	oscillatory pressure, $[FL^{-2}]$
R	resistance, $[FL^{-5}T]$
s	Laplace variable used to denote the complex frequency $\sigma + i\omega$, $[T^{-1}]$
t	time, [T]
ζ	ratio of critical damping for structural mode, [-]
ϕ_n	modal displacement, [-]
ω	angular frequency, $[T^{-1}]$

Subscripts

a	accumulator
b	bubble
t	tank

INTRODUCTION

The characteristics of the Space Shuttle vehicle, in both the propulsion system and the structural system, provide considerably more possibilities for pogo instability than have been encountered on previous boost vehicles. In the case of the liquid propulsion system, the long oxidizer feedline results in the presence of several feedline hydraulic modes in the structural frequency range of interest, while the two primary oxidizer pumps introduce a significant hydraulic mode in the interpump duct. In the case of the vehicle structure, the multiple-body nature of the Shuttle configuration introduces significant coupling between lateral and longitudinal motions with the result that the number of structural modes that are candidates for instability is increased. In addition, the wide variety and size of payloads imposes a requirement for maintenance of acceptable system damping in the face of variability of the structural vibration modes.

These aspects of the Shuttle system have necessitated considerable effort being directed toward the suppression of possible pogo instability in accordance with existing NASA Space Vehicle Design Criteria (Ref. 1). This effort has been supported on a continuing basis by The Aerospace Corporation under a number of NASA contracts. Previous studies (Refs. 2 and 3) for NASA (Langley) treated the use of accumulators for pogo suppression on the Shuttle; a major conclusion (Ref. 3) was that the accumulator would have to be located at the high pressure oxidizer turbopump (HPOTP) inlet in order to suppress the possible modes of instability. A later study (Ref. 4), undertaken for NASA (Lewis), provided an assessment of a number of active suppression devices; in this study it was found that the performance of the selected active designs was comparable to that predicted for a representative accumulator (a passive device). Both of these studies were undertaken with a simplified pitch plane model of the Shuttle structural/propulsion system, involving an equivalent single engine to represent the three liquid engines.

Support of the pogo suppression effort has been continued under contract to NASA (JSC). The initial work performed during this latter contract is described in the present report. This work comprised two distinct efforts, first, the performance of a parametric study for an accumulator located at the HPOTP inlet, and second, the development of a multiengine pitch plane stability model. The parametric study was undertaken with an equivalent single-engine model and had the objective of providing design guidelines for the selection of the baseline accumulator design. The study is described in Section 1 of the report. The development of the multiengine analytical model was a natural evolution that would enable a more refined analysis of the pogo problem to be performed. The model and the initial stability results obtained with this improved representation of the system are described in Section 2. The presented results reflect a limited examination of the system that was carried out to obtain an initial picture of the stability situation. More extensive stability studies with the multiengine model are planned for the future.

1. PARAMETRIC STUDY OF HPOTP INLET ACCUMULATOR

The parametric analyses involved a helium-charged accumulator located slightly ahead of the inlet to the HPOTP. The analytical model employed in the studies is first briefly reviewed, the numerical input data are then noted, and the analyses treating the sensitivity of the system stability to selected variations of the accumulator and system parameters are then described. Finally, a set of recommended design parameters for the accumulator are provided upon the basis of the study results.

1.1 ANALYTICAL MODEL AND PROCEDURES

The launch configuration of the Space Shuttle is depicted in Figure 1. The four-body configuration comprises the orbiter vehicle, an external tank, and two solid rocket boosters (SRB). The external tank contains a forward liquid oxygen (lox) tank and an aft liquid hydrogen tank for supply of the three main orbiter engines [each referred to as a Space Shuttle Main Engine (SSME)]. The lox is supplied to the orbiter vehicle via a long feedline segment that runs along the outside of the external tank. For the analysis of the pogo problem on the Shuttle, the elements of the liquid propulsion system associated with the lox circuit are of primary interest. The hydrogen system is viewed as a less likely contributor to a potential instability and has been omitted from the analytical representation. The feedsystem is shown schematically in Figure 1. For the purpose of preliminary analysis of the pogo problem a simple pitch plane single-engine model of these elements had been constructed in 1973. This model was initially used in the study of Ref. 3 and subsequently in the study of Ref. 4. This model is shown schematically in Figure 2 representing a lox tank, a lox feedline (one section that represents the longitudinal run along the external tank and one lateral section), a low-pressure oxidizer turbopump (LPOTP), an interpump duct, an HPOTP with an accumulator near its inlet, a high-pressure discharge line, and a thrust chamber. To assure a good description of the higher organ-pipe

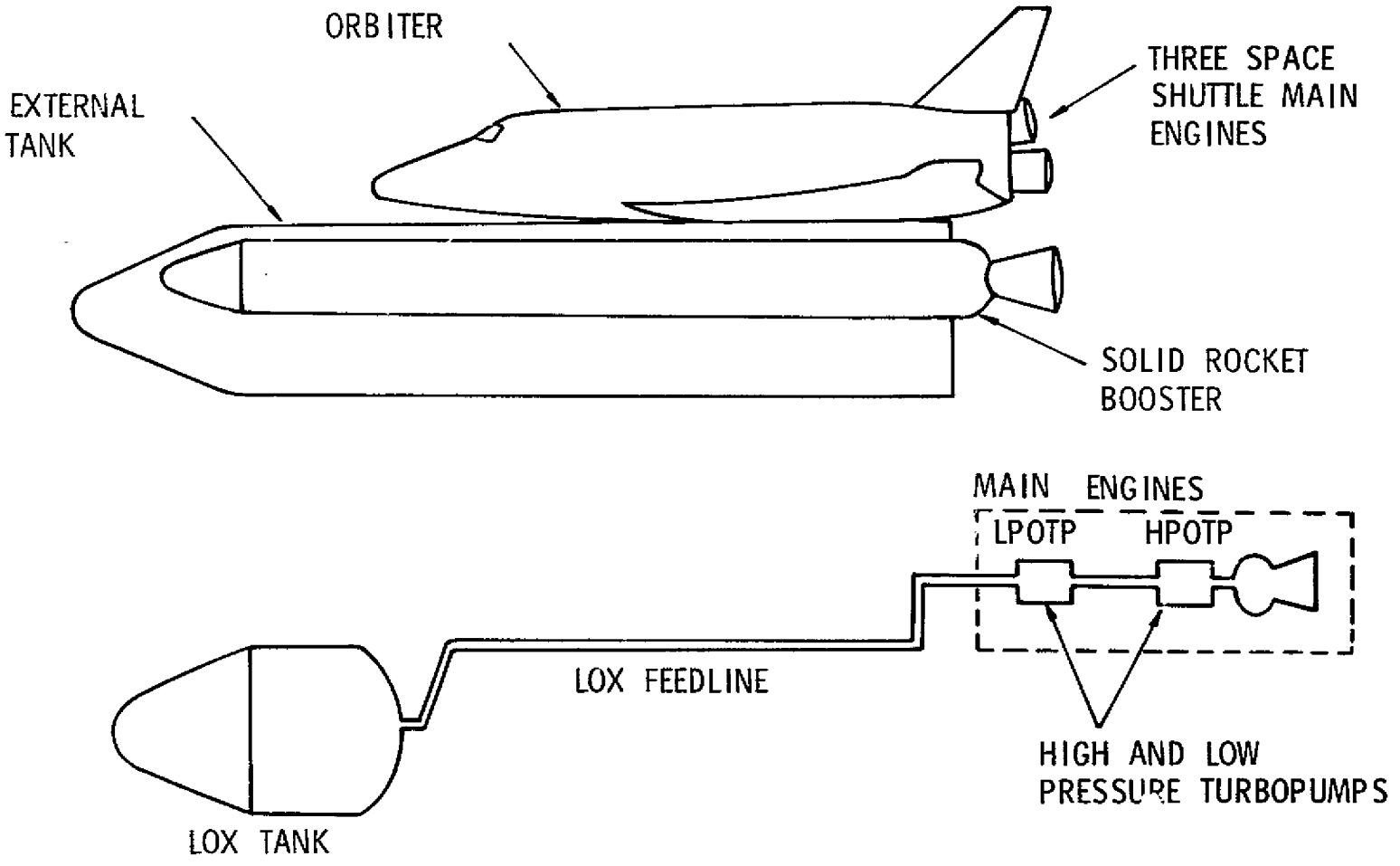

Figure 1. Schematic of Space Shuttle and Lox Circuit

modes of the feedline, the fluid flows in the feedline sections were represented by the exact solutions to the one-dimensional compressible flow equations. The fluid flow in the interpump duct was treated as incompressible since the associated wave transit time was relatively short compared to the structural response times of interest. Although this planar model represented a considerable simplification of the actual physical system, it was viewed as containing important elements of the pogo problem that are peculiar to the Shuttle, namely the presence of many feedline modes in the frequency range of interest, the presence of two pumps with a significant length of intermediate ducting internal to the engine, and the action of both longitudinal and lateral motions in the structural modes. The model used in the present parametric study was almost identical to the model used in the studies of Refs. 3 and 4; the only difference between the present model and the earlier version being the incorporation of finite separation between the accumulator and the pump (HPOTP). This finite separation, taken to be zero in the earlier studies, is dictated by engine geometric and functional considerations. The significance of the separation is two-fold: first, the separation influences the effectiveness of the accumulator; second, and more importantly, the separation introduces a new propulsion system mode of vibration that could provide an additional possibility for instability. This new mode is dominated by motion of the fluid between the accumulator and the cavitation compliance of the HPOTP. The potential for such a mode of instability has been demonstrated on the Delta vehicle (Ref. 5) so this consideration cannot be overlooked. Based upon discussions with Rocketdyne personnel, a distance of two line diameters was used in the analysis for the separation between the accumulator and the pump inlet flange. Regarding the other features of the analytical model, the structural motions of the system are represented by a single structural mode and tank dynamic outflow effects are included in the generalized force terms on the basis that the structural modes used in the analysis were developed with closed-bottom tanks (Ref. 2).

The eigenvalues and eigenvectors of the coupled structural/propulsion system were developed from the condition that the determinant of the equations for free vibration of the coupled system vanishes. The determinantal condition yielded a transcendental equation for the eigenvalues. The solutions of this equation were determined with the use of an iterative root-finding subroutine (Ref. 6) that used the input structural mode frequency and previously calculated propulsion-system frequencies as initial guesses.

To account for uncertainties in the system definition and modeling, the input structural mode frequencies were allowed to vary through a ±15% range about the nominal value. This degree of variation was judged to be a reasonable initial estimate to cover the worst case conditions in terms of the proximity of the structural and propulsion resonances.

1.2 NUMERICAL INPUT DATA

1.2.1 Structural Mode Data

The structural modes used in this initial parametric study and the two previous studies (Refs. 3 and 4) were taken from data generated by Rockwell International/Space Division for an early vehicle configuration (designated M89B) that was current in early 1973. The data comprised the frequencies and mode shapes of the first hundred pitch plane vibration modes of the vehicle at five specific flight conditions. The data also included the lox tank-bottom displacements and pressures associated with the structural modes. In Refs. 3 and 4 the stability of the basic system (i.e., no accumulators) was studied at three of the provided flight events, namely, liftoff, after-SRB separation and end-burn conditions. The modes used in those analyses had frequencies of up to 30 Hz and were selected upon the basis of the structural gain, G_e for longitudinal motions of the engine

$$G_e = \phi_e^2/M$$

where ϕ_e is the modal amplitude of the engine in the longitudinal direction and M is the generalized mass of the structural mode. In the present analysis

the more critical of these modes were employed. As in the previous studies, a 0.01 fraction of critical viscous damping was assigned to each structural mode.

Regarding the assignments of the structural mode amplitudes the elements of the engine (i.e., LPOTP, HPOTP and thrust chamber) were given identical motions. The corner at the aft end of the longitudinal feedline segment (point 2 in Figure 2) and the corner ahead of the LPOTP (point 3 in Figure 2) were also assigned identical motions. These assignments were necessary since the modal data did not provide a sufficient description of the propulsion system elements. The modal amplitude ϕ_e of the equivalent single engine was related to the modal amplitudes ϕ_{ei} of the individual engines by the equation

$$\phi_e^2 = \frac{1}{3}\sum_i \phi_{ei}^2$$

thereby maintaining the same net generalized force due to the engine thrust perturbations associated with motion of the engines. A similar procedure was applied to obtain an equivalent modal tank-bottom pressure excitation P_t. The relationship between P_t and the corresponding modal data P was

$$P_t = \frac{P}{3\phi_e}\sum_i \phi_{ei}$$

which gave the same net generalized force due to the engine thrust perturbations associated with the tank-bottom pressure.

1.2.2 Propulsion System Parameters

The cross-sectional areas and lengths of the various lines were based upon available Space Shuttle design data. The resistance and inertance of the lines, pumps, engine, and thrust chamber were developed from the basic data given in the SSME Engine Dynamic Model (Ref. 7) and from information in a previous pogo study (Ref. 2). Values for the cavitation bubble

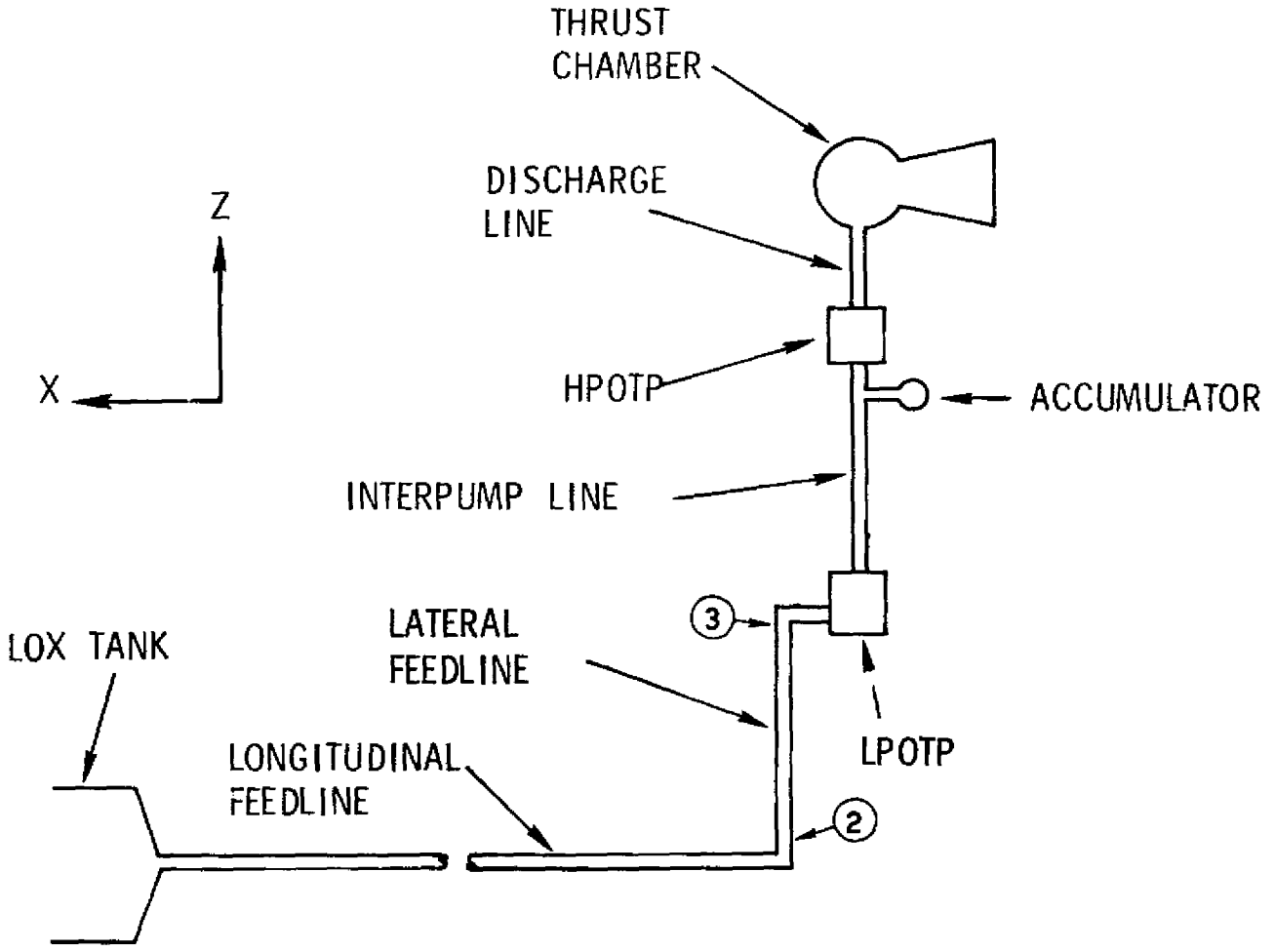

Figure 2. Schematic of Single Equivalent Engine Model

compliance (volume change per unit pressure change) at the pump inlets and for the pump gains were developed from available operating data. The compliance (C_b) estimates were made using the results presented in Ref. 2 (obtained from the "stay-time" method of Ref. 8). The pump gain (m+1) is related to the compliance based upon the following relationship derived from unpublished Titan and Delta vehicle studies:

$$(m+1) = 1 + 3000\,\rho g\, C_b/A_{in}$$

when ρ is the density of the fluid, g is the gravitational constant and A_{in} is the flow area at the inlet of the pump. The variations with flight time of the estimated nominal values of the compliance and gain parameters are illustrated in Figures 3 and 4. The data provided in Ref. 2 also enabled estimates to be made of upper and lower bound values of the compliance for use in sensitivity studies. The nominal, maximum and minimum values of compliance, and the corresponding pump gains, are provided in Table 1 for the liftoff, max dynamic pressure (max Q), after-SRB-separation, t = 254 sec and end-burn conditions.

1.3 STABILITY ANALYSIS

For the sake of completeness the stability results that had been obtained previously in Refs. 3 and 4 for the basic system (i.e., no accumulator) are briefly reviewed. The results obtained in the present study with the HPOTP inlet accumulator are then discussed and the resulting recommendations for the design parameters of the accumulator are provided.

1.3.1 Stability of System Without Suppression

Three flight events were analyzed in the previous work of Refs. 3 and 4. These events were the liftoff, after-SRB-separation and end-burn conditions. Instabilities had been predicted for each case in the absence of suppression. At the liftoff and after-SRB-separation events, the instability involved coupling between the low-frequency structural mode (designated L1 and A1, respectively, for the two events) and the corresponding fundamental

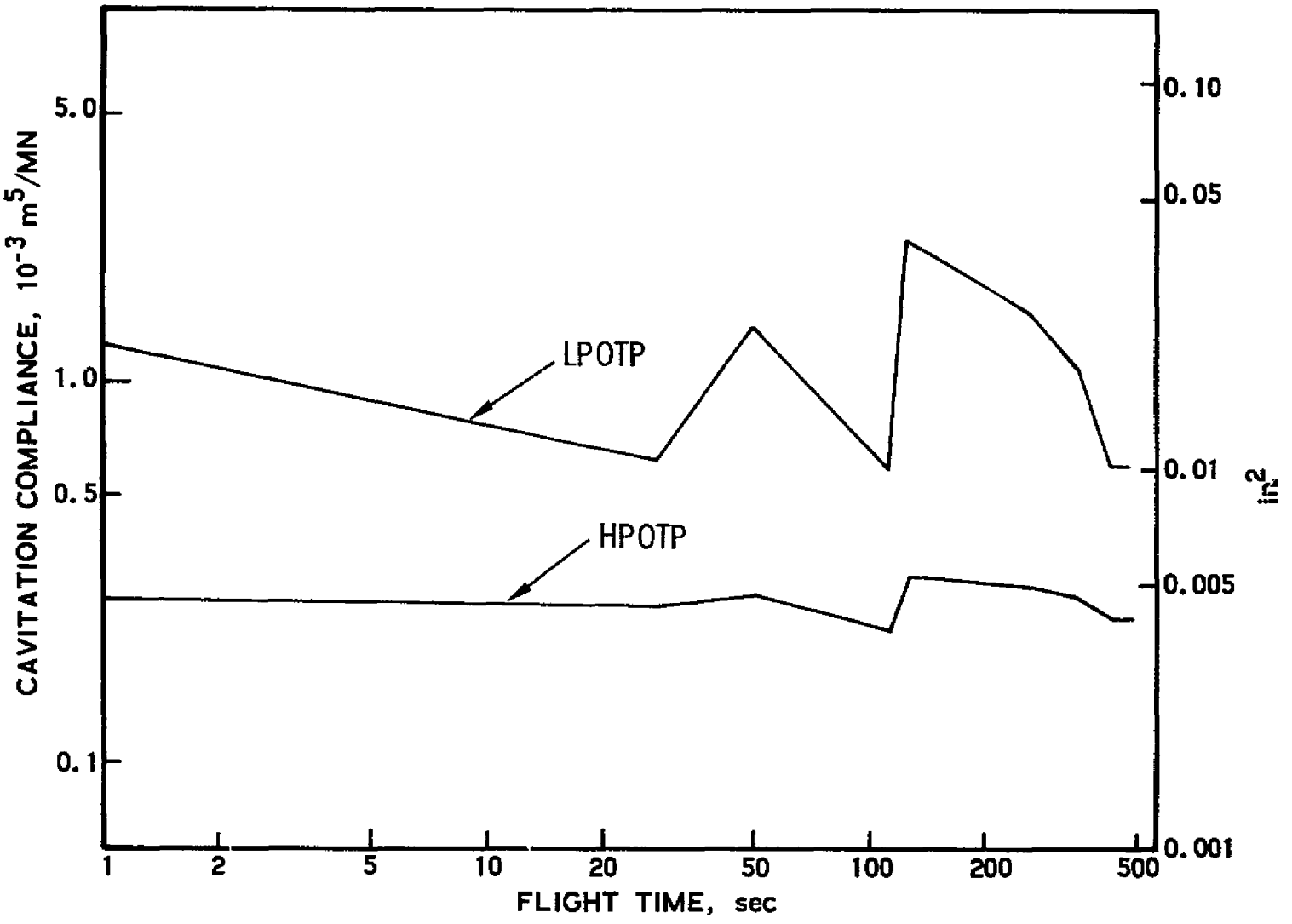

Figure 3. Variation of Nominal Pump Inlet Cavitation Compliance

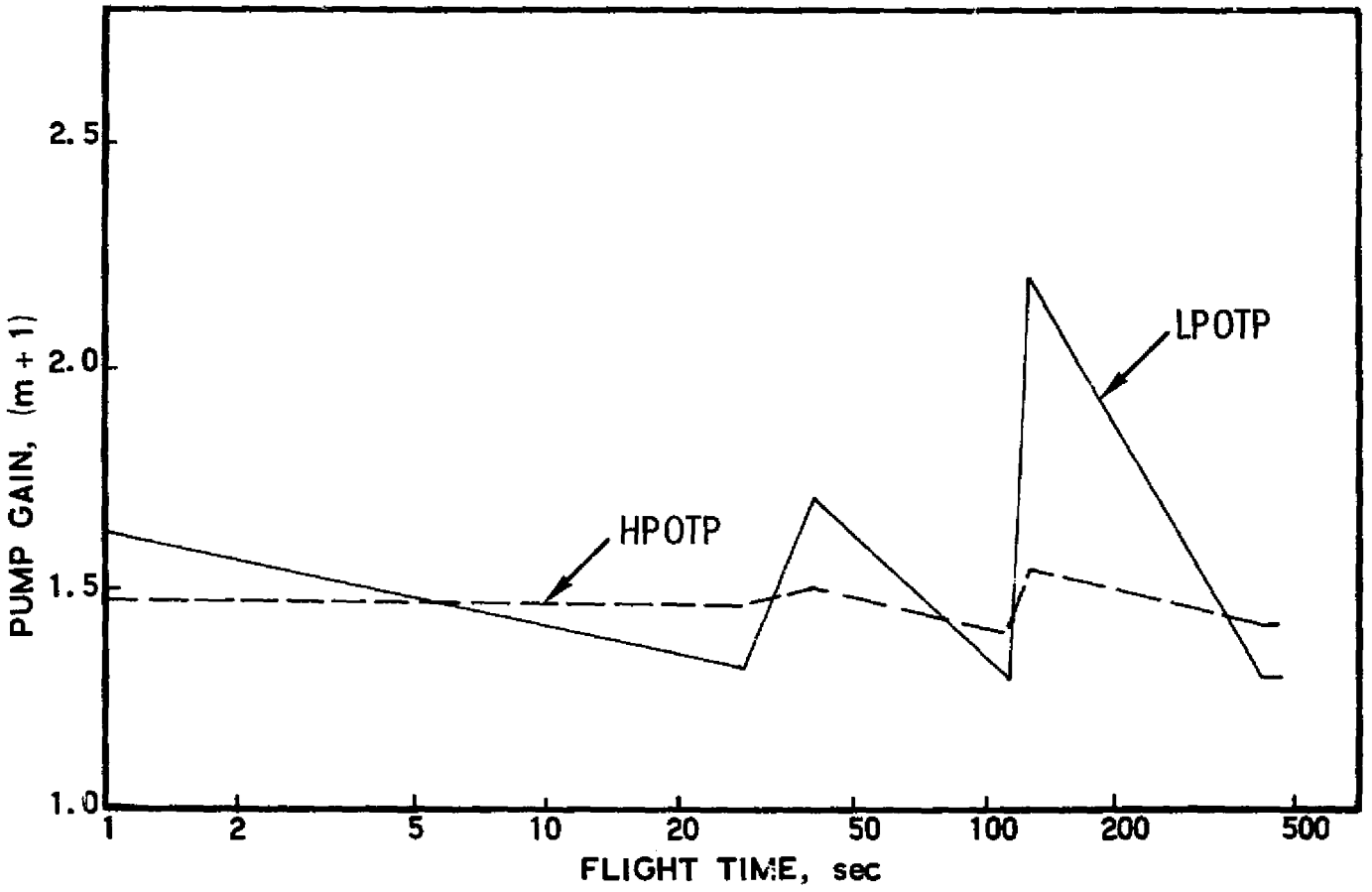

Figure 4. Variation of Nominal Pump Gain

propulsion system mode. At end-burn the instability involved coupling between the thirty-fifth structural mode (designated E35) and the interpump mode of the propulsion system. The predicted variation of the system damping ratio (that is, fraction of critical viscous damping for the system) for these three cases (over the assumed ±15% variation in structural mode frequency) is shown in Figures 5 and 6.

1.3.2 System with HPOTP Inlet Accumulator

The general effect produced by the introduction of a purely compliant accumulator (i.e., zero inertance and resistance) with zero separation from the HPOTP had been examined in Ref. 3. The present analysis is concerned with the effect of finite separation and the sensitivity of the accumulator performance to variations in the following system parameters:

a. Accumulator resistance
b. Accumulator inertance
c. Accumulator volume
d. Pump gain

For the purpose of the study a helium-charged accumulator was taken to be located at two line diameters ahead of the inlet flange of the HPOTP. Since the study was primarily concerned with the sensitivity of the accumulator performance to parametric variations, the analyses only dealt with the structural modes that had been found to be unstable for the system without suppression (i.e., the L1, A1 and E35 modes). In the previous investigation of Ref. 3, it had been found that the presence of an accumulator did not introduce stability problems with additional structural modes.

1.3.2.1 Accumulator/Pump Separation

The effect of finite separation on the effectiveness of the accumulator in eliminating the instabilities predicted for the basic system was first examined. From a modeling standpoint, the separation provides a significantly large inertance for the propellant flow path beginning at the entrance to

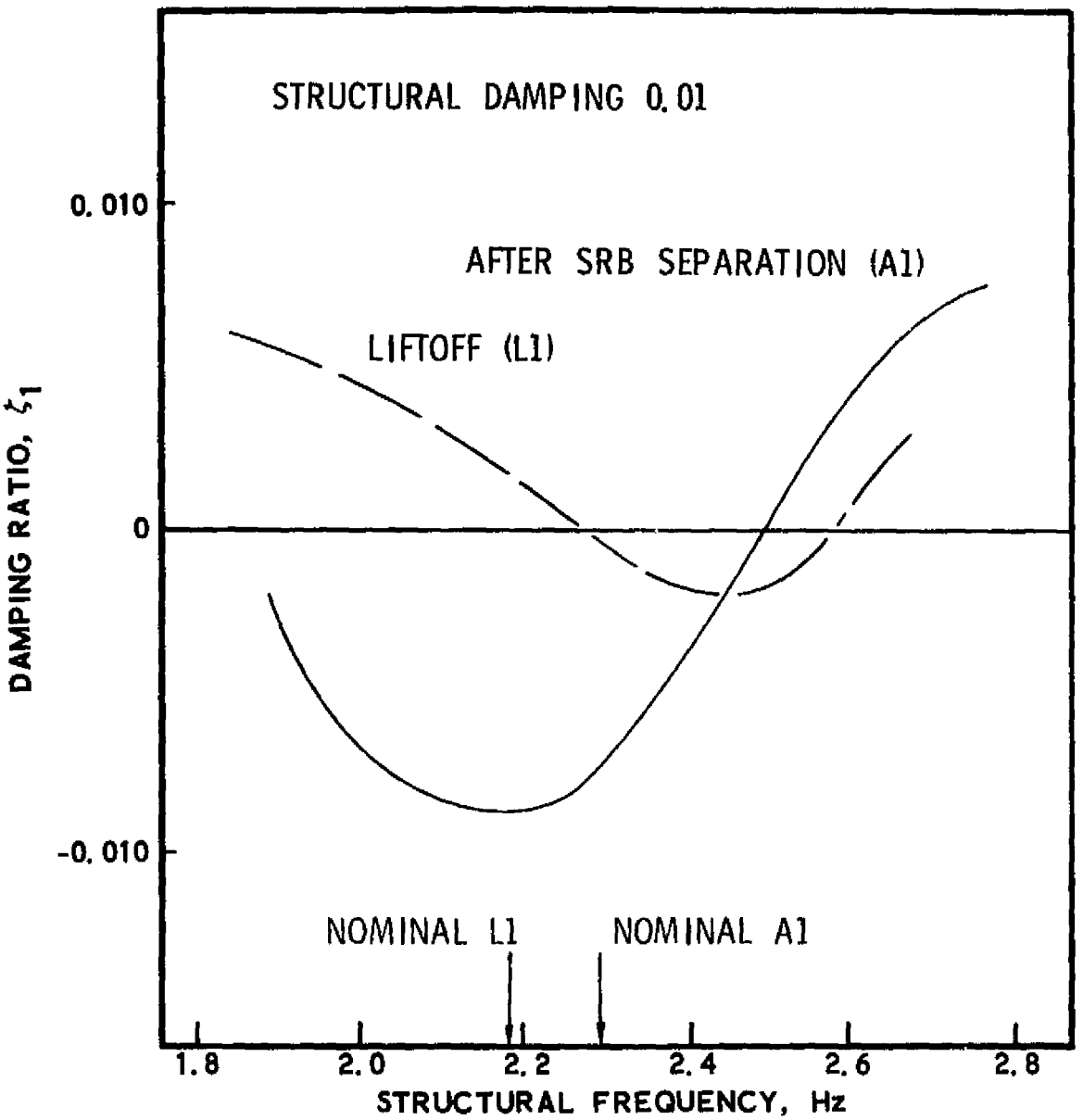

Figure 5. System Damping Without Pogo Suppression; Low-Frequency Modes at Liftoff (L1) and After SRB Separation (A1)

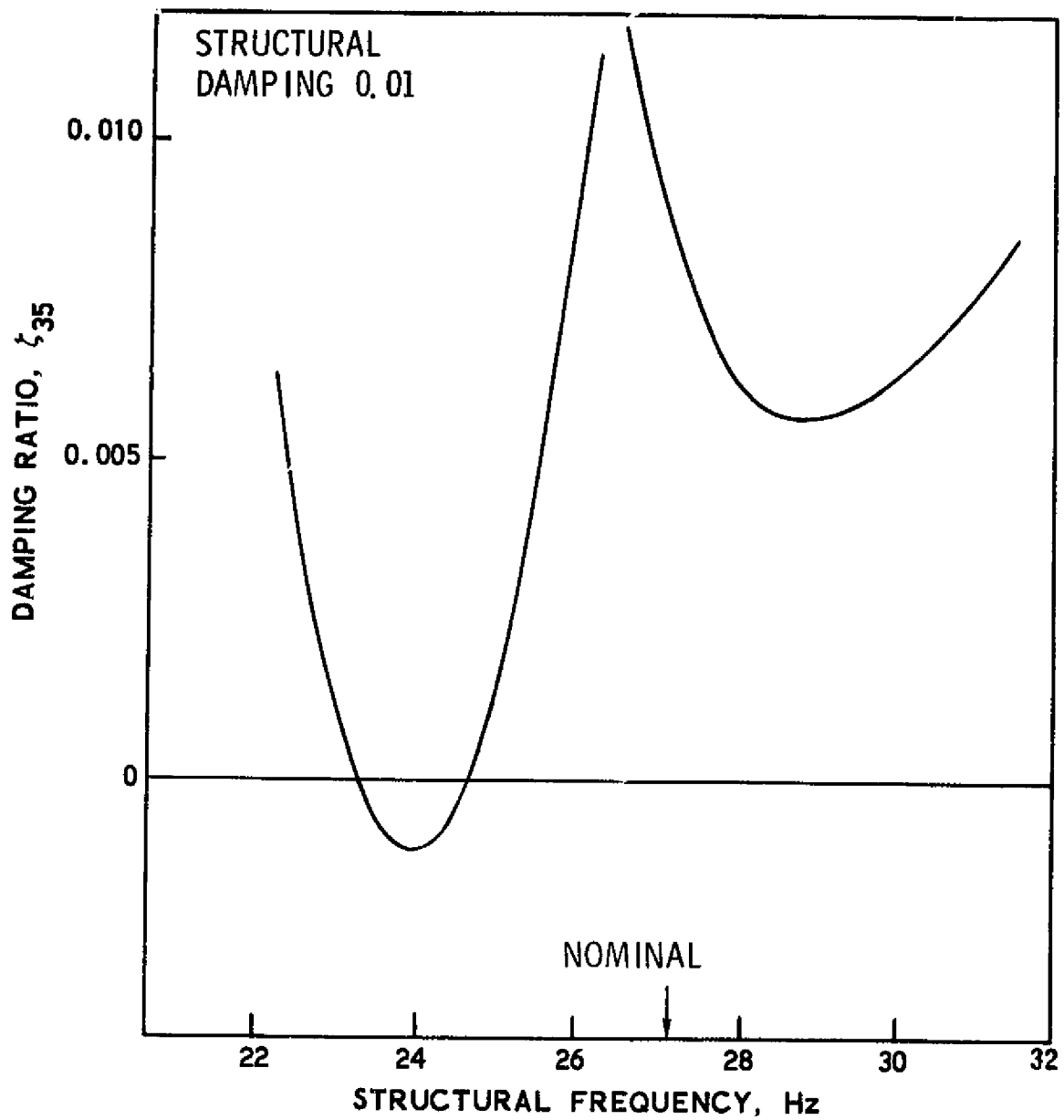

Figure 6. System Damping Without Pogo Suppression; End-Burn Mode E35

the accumulator and ending at the cavitation compliance of the HPOTP. The consequence of separation was determined by direct comparison of system stability levels obtained for a purely compliant accumulator without separation and for a purely compliant accumulator located two diameters ahead of the inlet flange. The comparison indicated that the two-diameter physical separation produced (1) a minor reduction in the effectiveness of the accumulator in the lower frequency modes (see Figure 7 for the A1 mode) and (2) a more significant reduction in the accumulator effectiveness in the higher frequency E35 mode, as shown in Figure 8. In the latter case, however, it will be noticed that the minimum calculated damping ratio was maintained above a 0.005 level even with the degradation of accumulator performance; thus the damping gain margin remained above 6dB (Ref. 1).

The possibility of an instability being introduced by the presence of the new propulsion system mode associated with the fluid between the accumulator and the pump cavitation compliance was next examined. This new "separation" mode can be viewed as the vibration of the fluid mass on the gas springs provided by the accumulator and the cavitation bubble of the HPOTP. Consequently the resonant frequency of the mode can be estimated with the formula

$$f_{sep} \approx \frac{1}{2\pi} \left(\frac{1/C_a + 1/C_{b2}}{L_a + L_s} \right)^{1/2}$$

where L_a, L_s denote the inertance of the accumulator and the fluid between the accumulator and the pump cavitation, respectively; and where C_a, C_{b2} denote the compliance of the accumulator and of the cavitation bubble at the pump inlet, respectively. For the purpose of the calculations, the inertance values were taken to be

$$L_a = 0.034 \text{ MN s}^2/\text{m}^5 \ (0.002 \text{ sec}^2/\text{in.}^2)^*$$

$$L_s = 0.043 \text{ MN s}^2/\text{m}^5 \ (0.0025 \text{ sec}^2/\text{in.}^2)$$

*Inertance in SI units is based upon use of a volume flow; in English units, weight flow is employed.

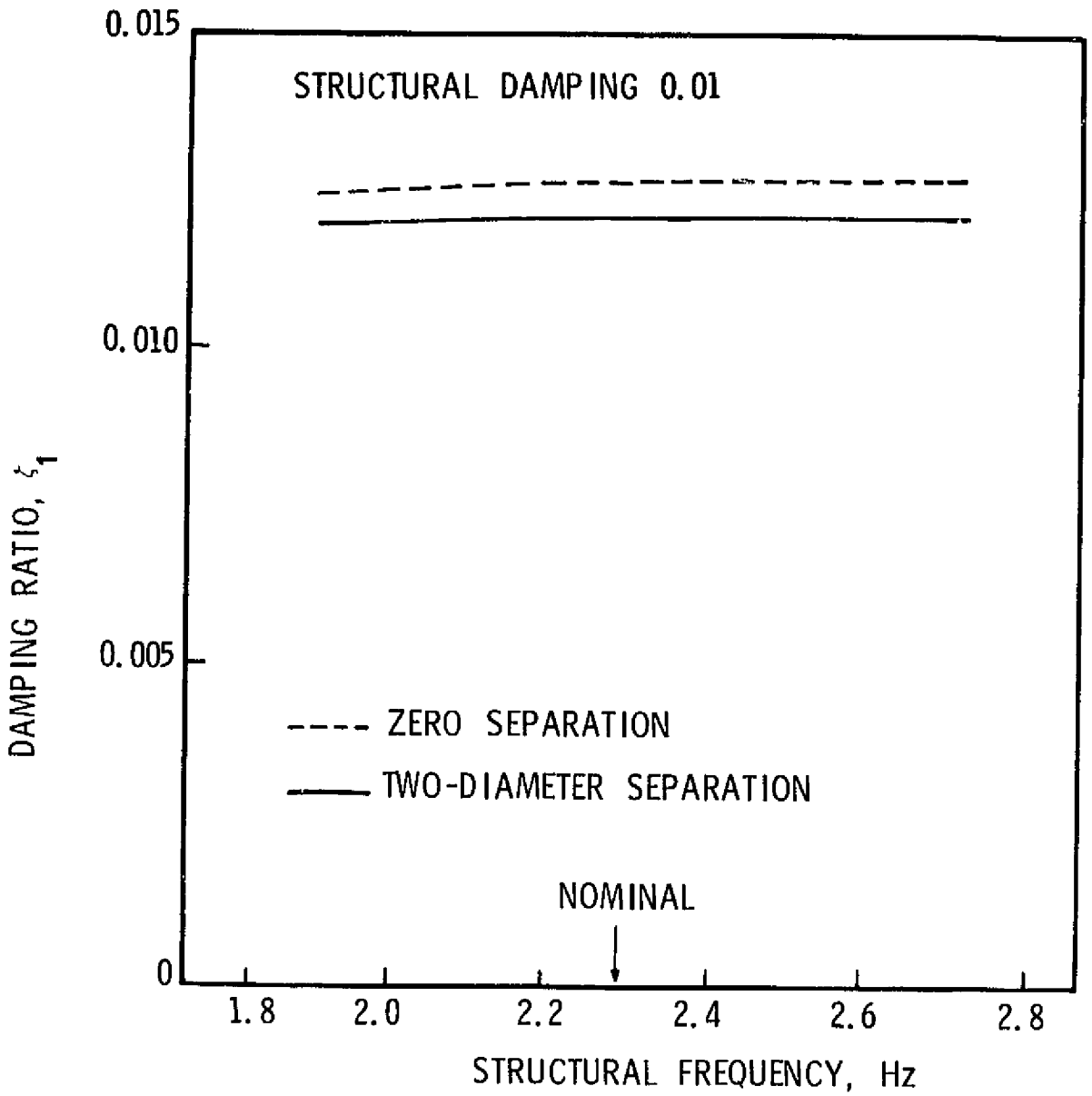

Figure 7. Effect of Accumulator Separation on System Damping: 0.028 m^3 (1 ft^3) Compliant Accumulator, Low-Frequency Mode After SRB Separation (A1)

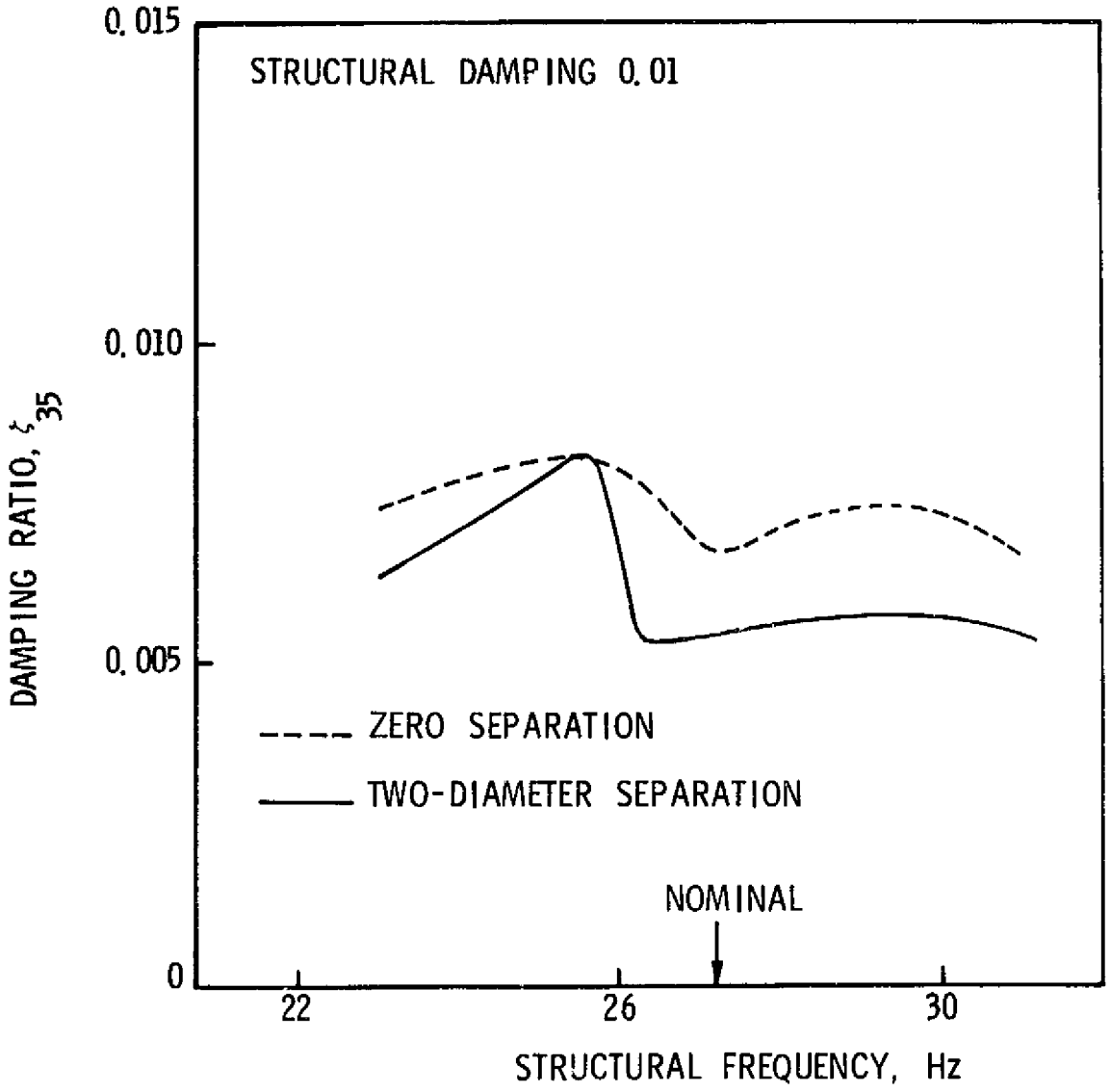

Figure 8. Effect of Accumulator Separation on System Damping: 0.028 m^3 (1 ft^3) Compliant Accumulator, E35 Mode at End Burn

The selected accumulator inertance was viewed as a reasonable upper bound based upon the geometric constraints on the accumulator inlet; the line inertance was estimated from the geometry of the pump inlet and the two-diameter separation. Taking an accumulator helium volume (per engine) of 0.028 m^3 (1 ft^3), the estimated nominal HPOTP inlet cavitation bubble compliance, and considering the end-burn flight condition, the frequency of the separation mode was estimated to be about 38 Hz. This value was above the frequency range being considered in the analysis. It was decided to cause a reduction in the frequency of the separation mode to 25 Hz, near which instability had been exhibited by the E35 mode in the system without suppressors (Figure 6). This reduction was achieved by increasing the HPOTP compliance from the nominal end-burn level of 0.00024 m^5/MN (0.004 $in.^2$) to a value of about 0.0006 m^5/MN (0.01 $in.^2$), a value well below the maximum value of 0.0014 m^5/MN (0.023 $in.^2$) (see Table 1). Stability analyses were then run with the E35 mode and the resulting system damping as shown in Figure 9 reveals a system instability with the damping ratio reaching a low of -0.007 within the imposed ±15 percent variation of structural mode frequency. For comparison the corresponding results for a 0.028 m^3 (1 ft^3) compliant accumulator without separation are also shown in the figure. The source of the instability is the presence of the separation mode which has coupled in a destabilizing manner with the E35 structural mode. It should be noted that the preceding results were obtained for accumulators that had no resistance. In the next section of the study the effect of accumulator resistance upon both this instability and those predicted in the absence of an accumulator will be examined.

1.3.2.2 Accumulator Resistance

On the basis of studies for the Delta Stage I vehicle (Ref. 5), as well as physical insight, it was known that resistance in the accumulator could improve the stability involving the separation mode. First, the effect of adding resistance on this mode in the Shuttle system was examined. Stability analyses were run for the E35 mode with the same parameters used for the zero-resistance case (results appear in Figure 9) except that

Table 1. Values for Pump Gain and Pump-Inlet Cavitation Compliance

Item \ Case	Liftoff (t = 0)	Max Q (t = 50)	After SRB Separation (t = 116)	t = 254 sec	End Burn (t = 480)
LPOTP Gain, $m_1 + 1$	1.63/2.23/1.10*	1.70/2.41/1.14	2.2/3.4/1.3	1.78/2.53/1.15	1.31/1.64/1.0
HPOTP Gain, $m_2 + 1$	1.48/3.64/1.24	1.50/3.7/1.25	1.54/3.85/1.27	1.51/3.77/1.26	1.42/3.4/1.21
LPOTP Compliance, C_{b1}					
$10^{-3} m^5/MN$(1)	1.2/2.4/0.18	1.41/2.7/0.26	2.3/4.6/0.59	1.47/3.0/0.30	0.59/1.2/0
(10^{-2} in.^{2})	(2.0/4.0/0.3)	(2.4/4.6/0.44)	(3.9/7.8/1.0)	(2.5/5.0/0.5)	(1.0/2.1/0)
HPOTP Compliance, C_{b2}					
$10^{-3} m^5/MN$	0.27/1.5/0.14	0.29/1.5/0.14	0.30/1.6/0.15	0.29/1.5/0.14	0.24/1.4/0.12
(10^{-2} in.^{2})	(0.45/2.5/0.23)	(0.48/2.5/0.23)	(0.51/2.7/0.25)	(0.48/2.6/0.24)	(0.40/2.3/0.20)

*nominal/maximum/minimum values provided for all entries

(1) Compliance in SI units is a volume change per unit pressure change; in English units, it is the weight of liquid displaced per unit pressure change.

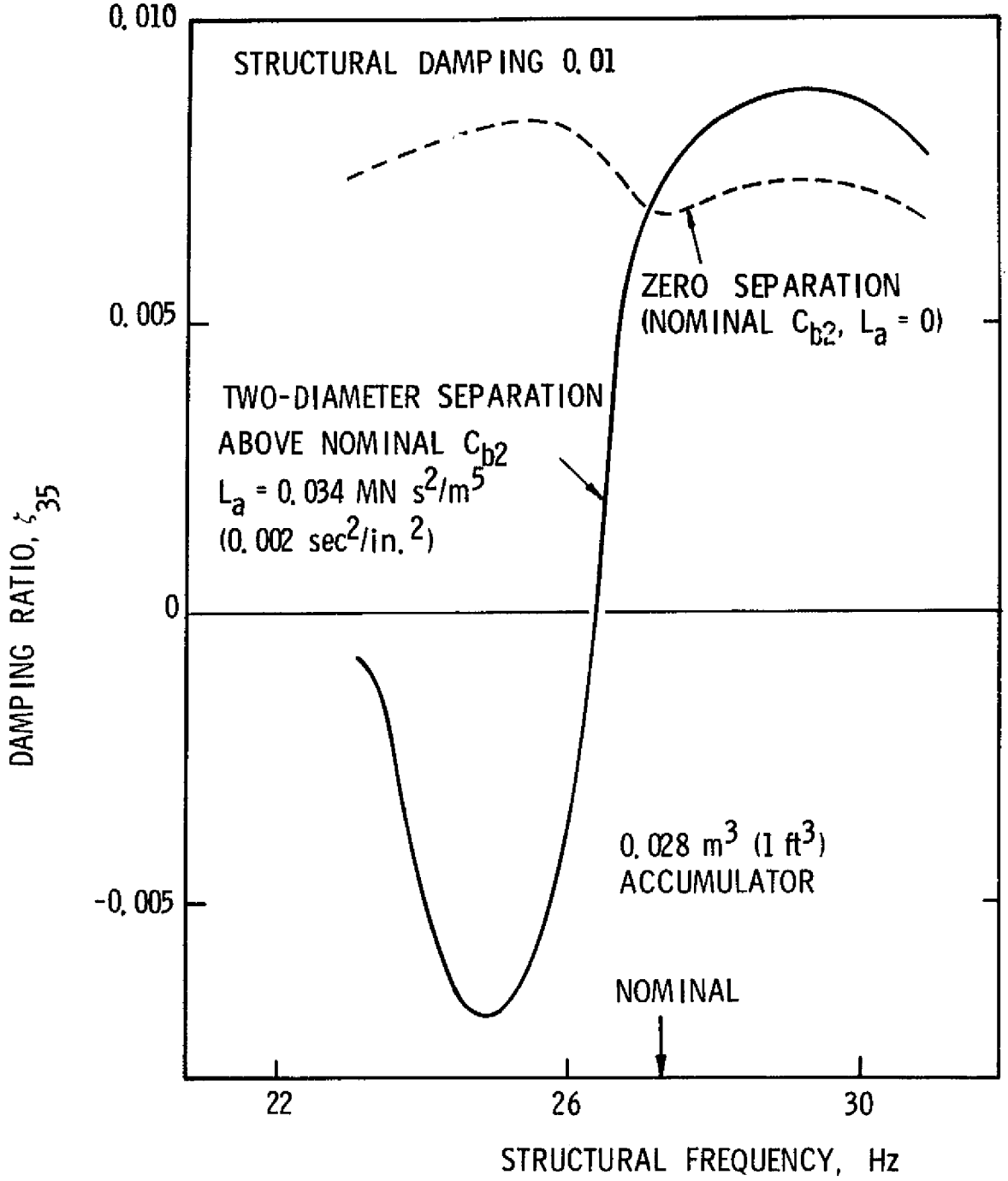

Figure 9. Instability Due to E35/Separation Mode Coupling: End Burn

accumulator resistances of up to 17 MN s/m^5 (1.0 sec/$in.^2$) are employed. The results of the calculations confirmed that accumulator resistance could be highly effective in eliminating the instability associated with the separation mode. This effect is illustrated in Figure 10, where the minimum calculated damping ratio (over the ±15 percent frequency range) is plotted versus the accumulator resistance. For example, a resistance value of 8.4 MN s/m^5 (0.5 sec/$in.^2$) effectively eliminates the instability, with diminishing returns for higher values of resistance.

The effect of accumulator resistance on the performance of the accumulator with nominal HPOTP compliance was next examined. In this instance, the separation mode, at about 38 Hz, was above the frequency range of interest. Stability analyses were run over the ±15 percent frequency ranges for the L1, A1 and E35 structural modes using accumulator resistances of up to 17 MN s/m^5 (1.0 sec/$in.^2$). The resulting predicted damping levels indicated some lessening in the effectiveness of the accumulator. The effect is illustrated in Figure 11 where the minimum damping ratios (over the ±15 percent frequency range) are plotted versus accumulator resistance for both the A1 and E35 modes. The results were calculated for a 0.057 m^3 (2 ft^3) volume accumulator with an inertance of 0.010 MN s^2/m^5 (0.0006 $sec^2/in.^2$). The resistance value of 8.4 MN s/m^5 (0.5 sec/$in.^2$), shown to be highly effective in Figure 10, produces what are judged to be tolerably small degradations of system damping.

1.3.2.3 Accumulator Inertance

A parametric study of the effect of the accumulator inertance was also examined with nominal HPOTP compliance to absent the separation mode. Stability analyses were run using inertance values up to 0.034 MN s^2/m^5 (0.002 $sec^2/in.^2$). The results indicated that these inertance levels had negligible effect on the performance of the accumulator in the low-frequency modes, however, a significant reduction in the effectiveness of the device was found in the higher frequency E35 mode. This latter effect is

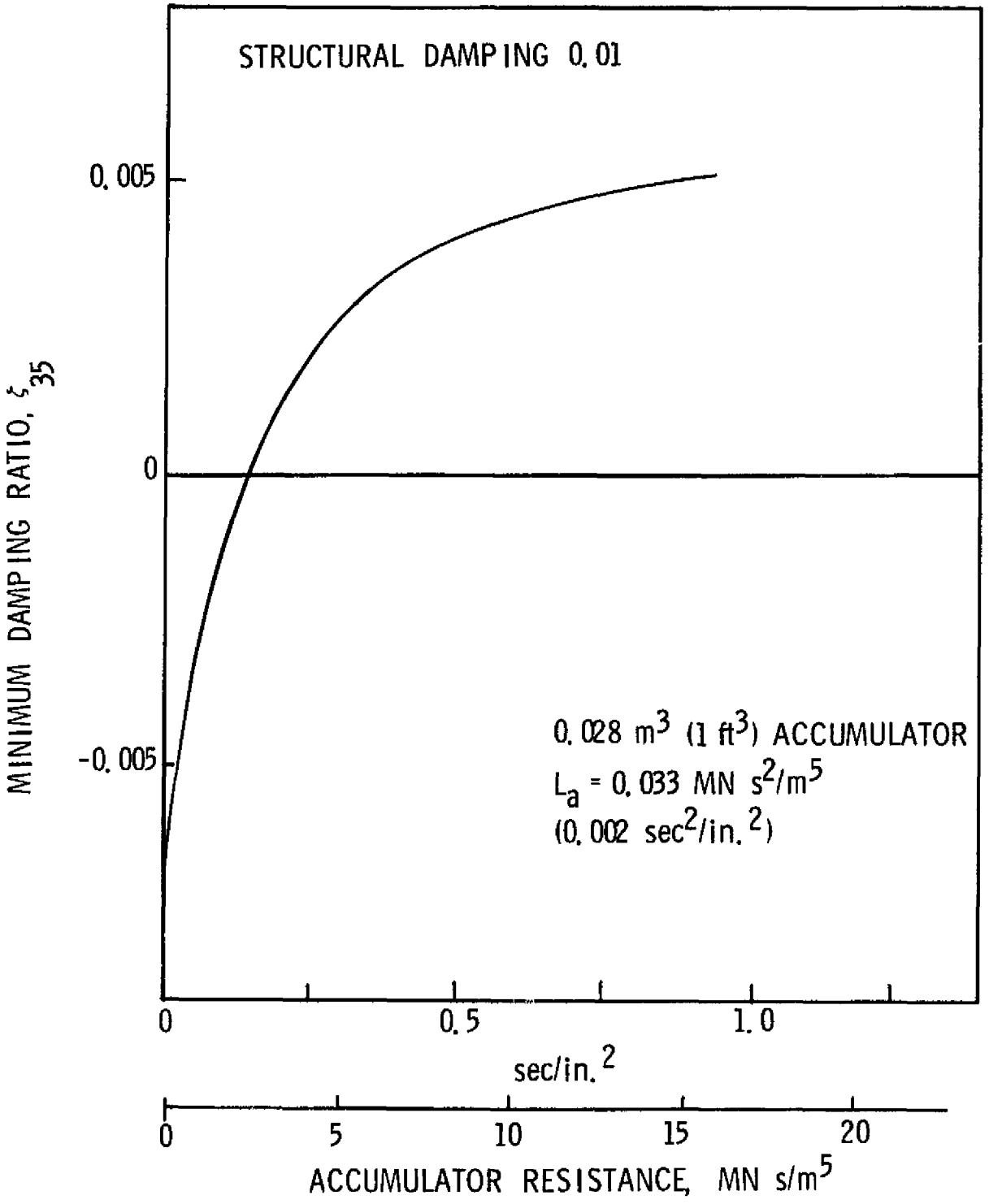

Figure 10. Effect of Accumulator Resistance on Stability of E35/Separation Mode: End Burn

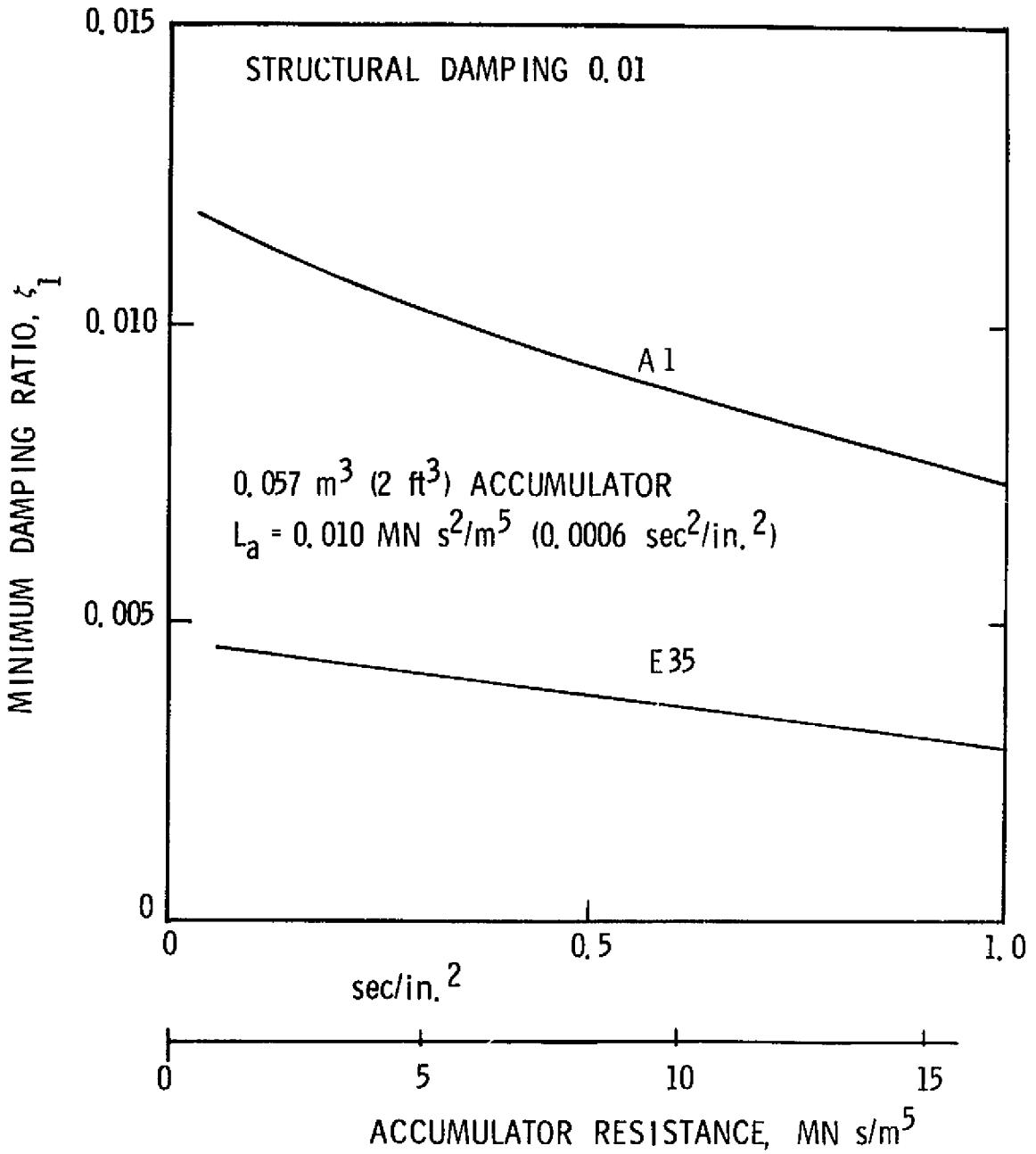

Figure 11. Effect of Accumulator Resistance on Stability of A1 and E35 Modes

illustrated in Figure 12 where the minimum calculated damping ratios for this mode (over the ±15 percent frequency range) are presented as a function of inertance, for accumulator volumes of 0.014, 0.028 and 0.057 m^3 (0.5, 1.0 and 2.0 ft^3). It is judged that the stability degradation with increasing accumulator inertance is tolerable for inertance values up to 0.017 MN s^2/m^5 (0.001 $in.^2$).

1.3.2.4 Accumulator Volume

The sensitivity of the accumulator performance to the volume of the accumulator is an item of considerable interest because of the increase to vehicle weight with increasing size of the accumulator. To investigate this sensitivity, stability analyses were run with the L1, A1 and E35 modes using accumulator helium volumes of 0.014, 0.028 and 0.057 m^3 (0.5, 1.0 and 2.0 ft^3). The results of the calculations indicated that the performance of the device in the low-frequency modes was highly sensitive to volume, whereas the performance was relatively insensitive to volume in the higher frequency E35 mode. The sensitivity in the low-frequency modes is illustrated in Figure 13, where the minimum damping ratio obtained for the L1 mode is plotted as a function of accumulator volume. The results are given for both zero accumulator resistance and a resistance of 17 MN s/m^5 (1.0 $sec/in.^2$). A dramatic decrease in the effectiveness of the accumulator is evident once the volume has dropped below about 0.028 m^3 (1 ft^3). This sensitivity to the accumulator volume is associated with the separation between the frequencies of the low-frequency structural mode and the fundamental propulsion system mode. In Figure 14 the variation of fundamental propulsion system mode frequency with accumulator volume is shown in conjunction with the ±15 percent tolerance band around the nominal structural mode frequency. It is seen that the propulsion mode frequency remains within the tolerance band for accumulator volumes below about 0.014 m^3 (0.5 ft^3). As the volume continues to increase above this level, separation between the frequencies increases and stability is enhanced. Clearly the volume requirement on the accumulator depends critically on the lower bound assumed for the frequency of the low-frequency structural mode. This matter will be dealt with again later in the report (e.g., see Figure 30).

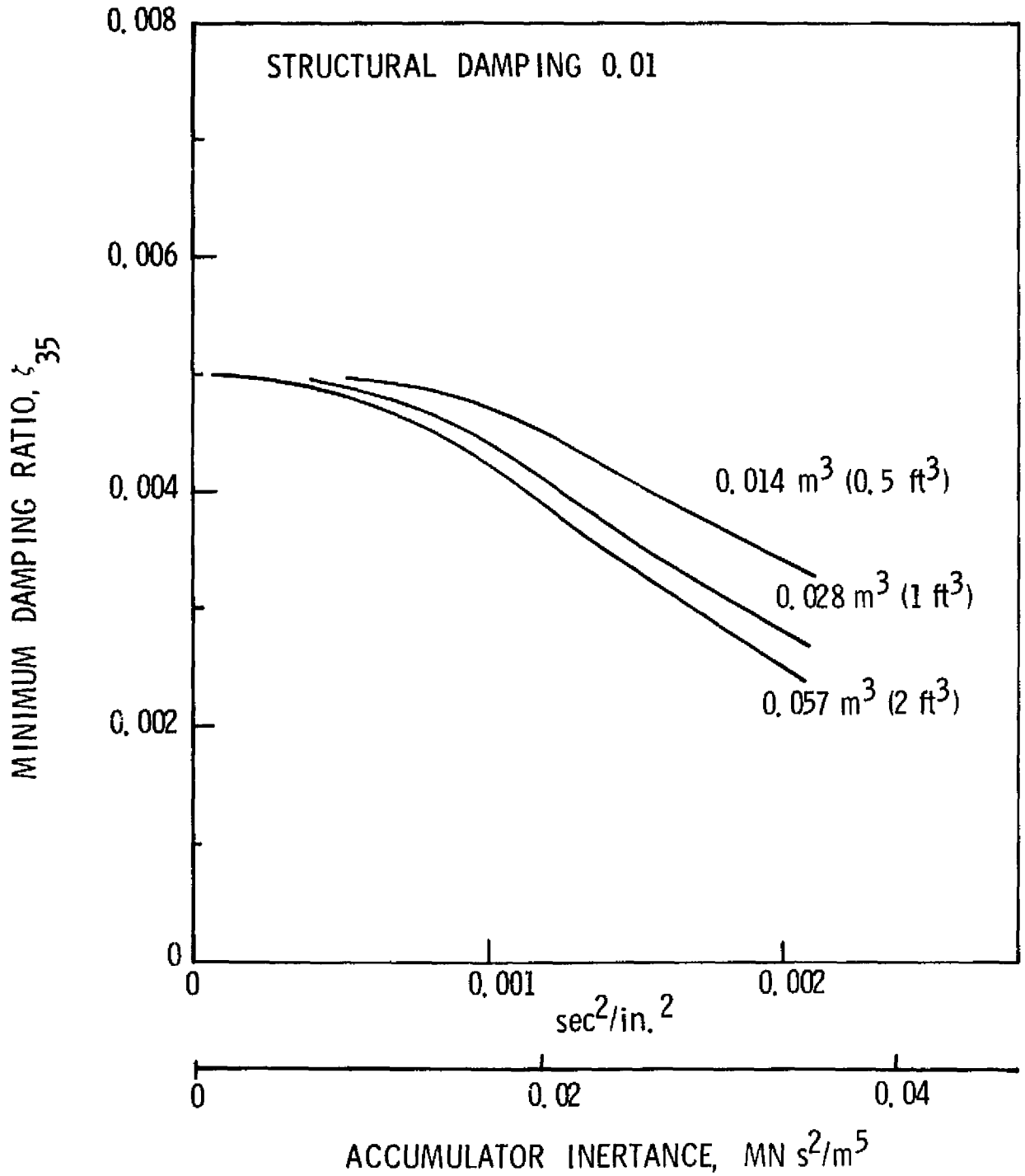

Figure 12. Effect of Accumulator Inertance on Stability of E35 Mode

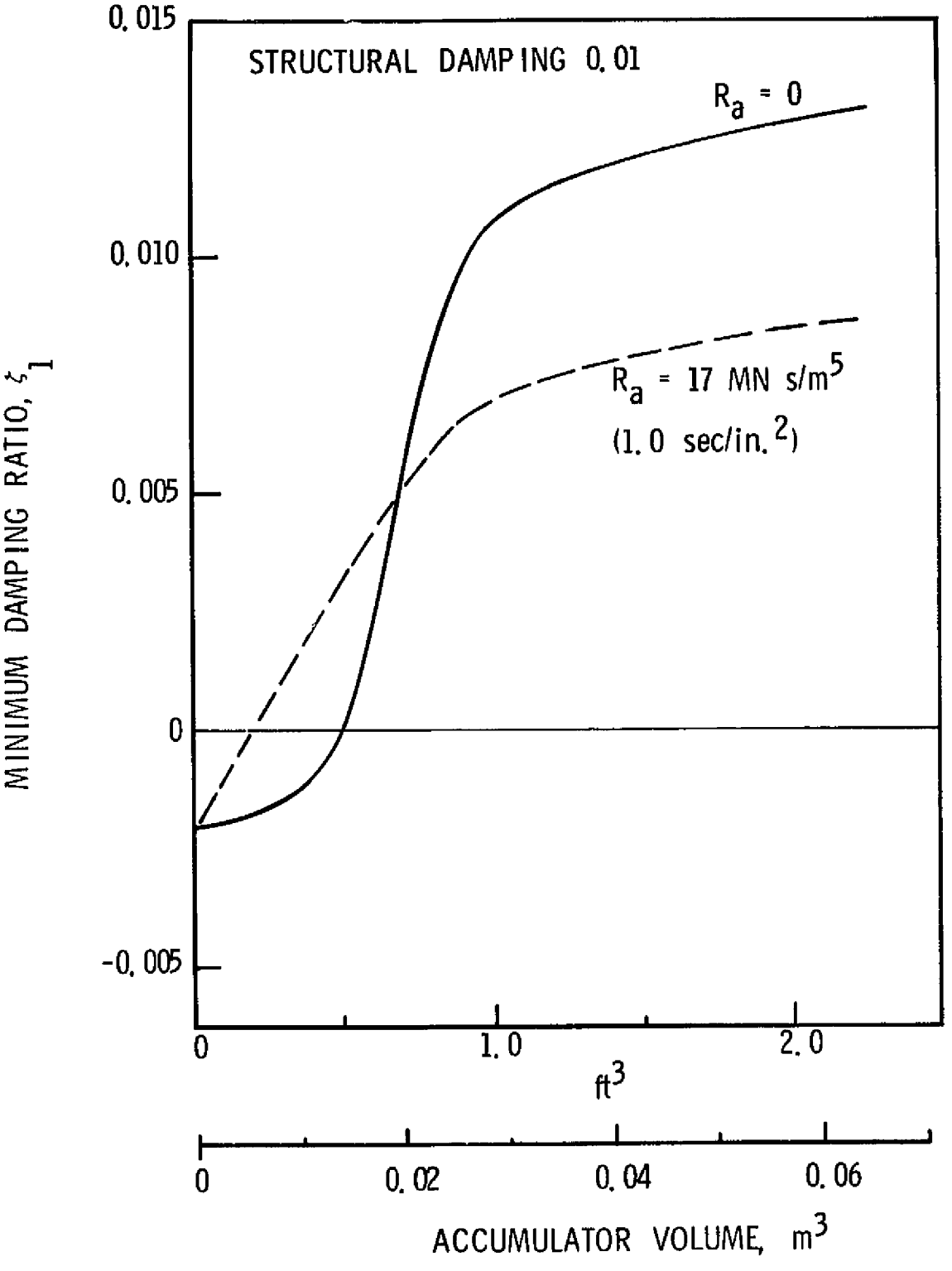

Figure 13. Minimum Damping Ratio Versus Accumulator Volume: Low-Frequency Mode at Liftoff (L1)

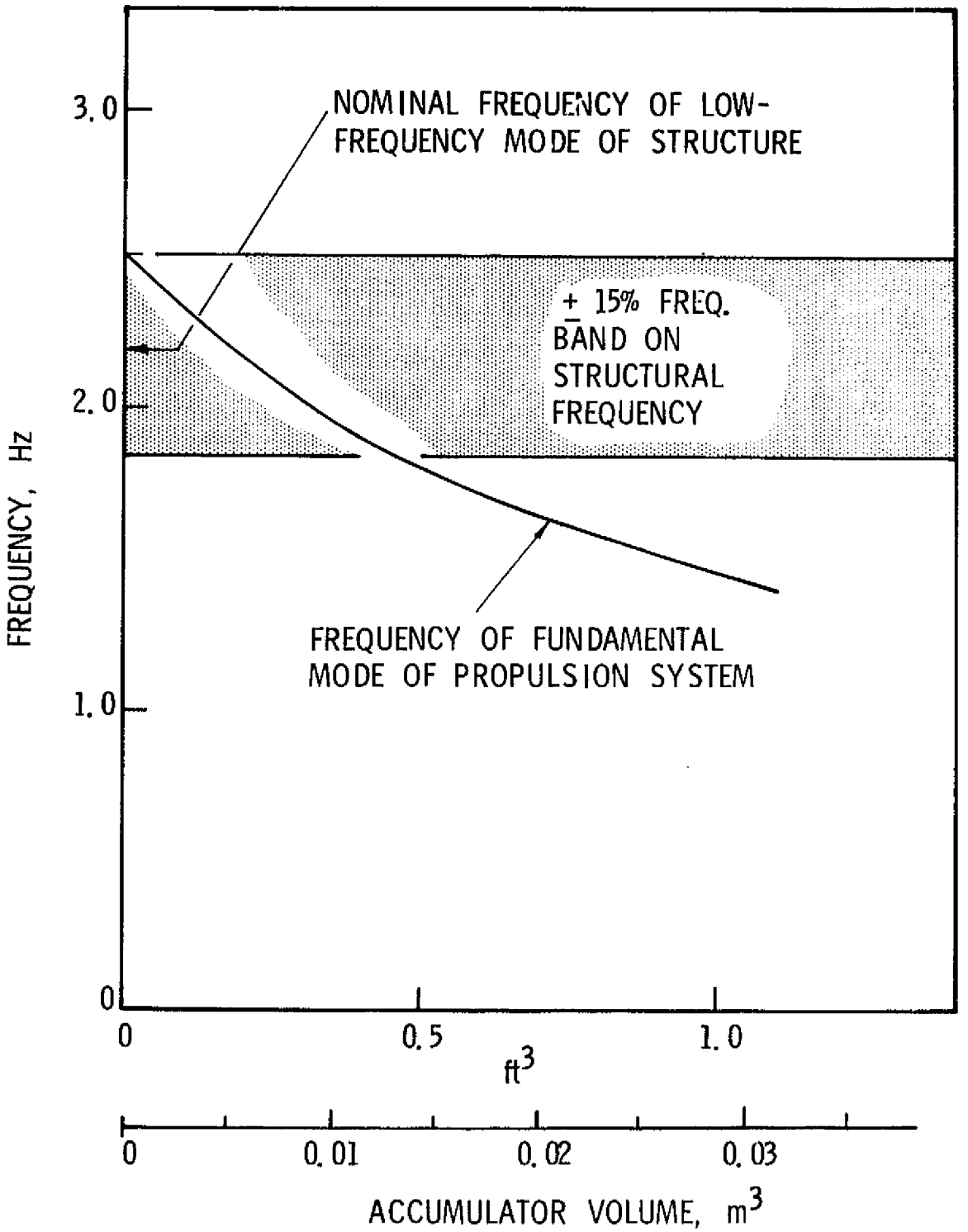

Figure 14. Relationship of Low-Frequency Propulsion and Structural Frequencies at Liftoff Versus Accumulator Volume

1.3.2.5 Pump Gain

Finally, the influence of pump gain on the stability of the system was examined. Stability analyses were performed for pump gains from a value of unity, as employed by Rocketdyne, up to the maximum values given in Table 1. The results of the analyses indicated a considerable sensitivity of the system stability in the low-frequency structural mode to pump gain. In the higher frequency E35 mode the system stability was found to be insensitive to the variations in the pump gain; this insensitivity occurs since the coupling involves the interpump mode of the propulsion system rather than a feedline type mode. The sensitivity in the low-frequency mode is illustrated in Figure 15, where the minimum calculated damping ratio (over the ±15 percent variation in structural frequency) for the L1 mode is plotted as a function of the product of the gains of the LPOTP and HPOTP pumps. Results are presented for accumulator volumes of 0.014, 0.028 and 0.057 m^3 (0.5 ft^3, 1.0 ft^3 and 2.0 ft^3). The nominal and maximum values of the pump gain product for the time of liftoff are identified on the figure.

To illustrate further the interplay between system damping, pump gain and accumulator volume the stability results are presented in a somewhat different format in Figure 16. In this figure, contours of constant system damping are presented as a function of both pump gain product and accumulator volume. The results clearly show that an accumulator with a volume of about 0.028 m^3 (1 ft^3) provides considerably more capability for maintaining high system damping for high pump gains than would a 0.014 m^3 (0.5 ft^3) volume device. The rapid increase in system damping with accumulator volumes above 0.014 m^3 (0.5 ft^3) occurs at this particular volume primarily because of the relationship of frequencies presented in Figure 14; that is, frequency coincidence occurs for the minimum structural frequency with the 0.014 m^3 (0.5 ft^3) accumulator volume and increased volume leads to frequency separation and thus increased system damping. If the low-frequency structural frequency were to be allowed to fall below minus 15 percent of nominal, the upward break in system damping in Figure 15 would

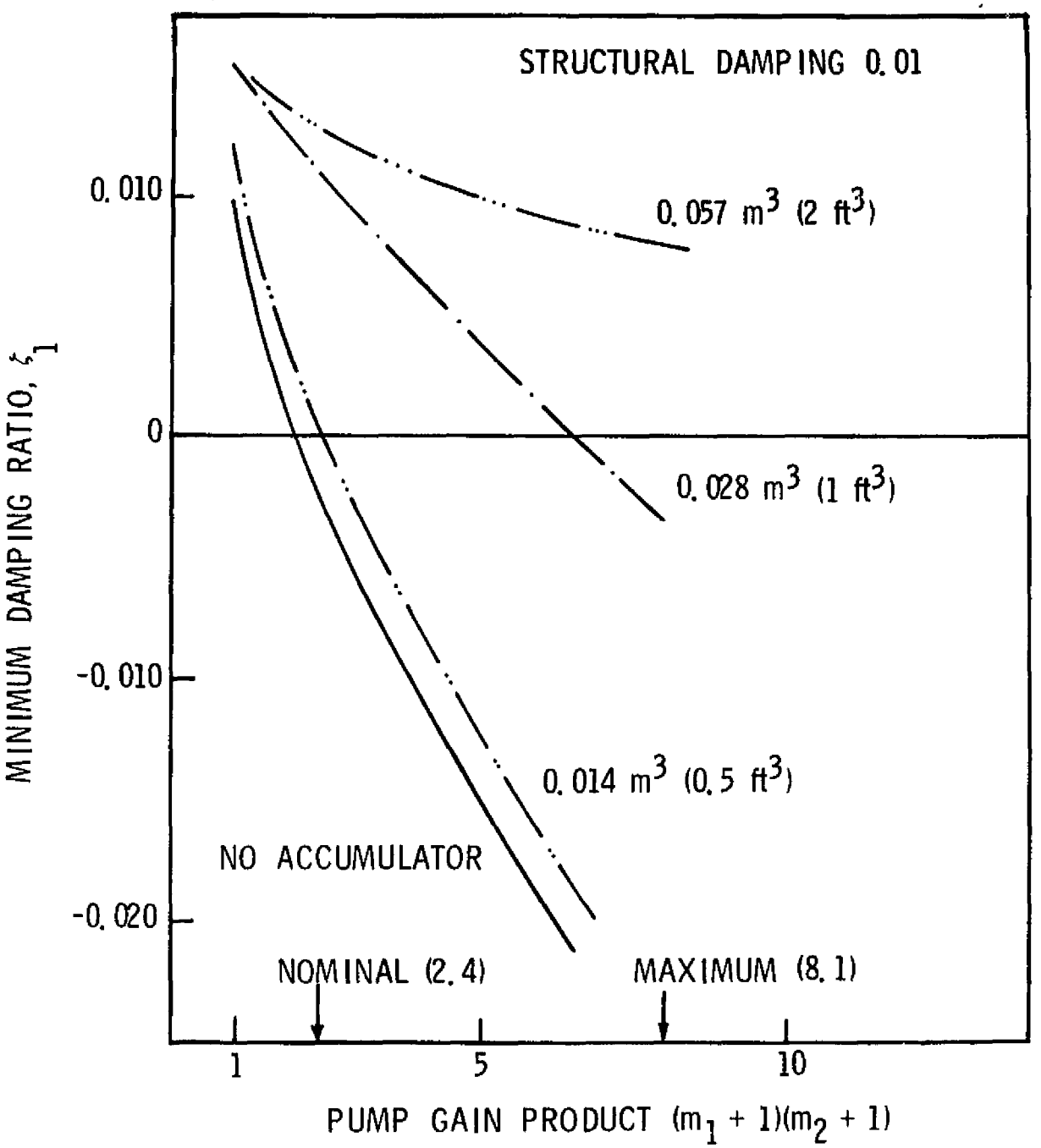

Figure 15. Damping of Low-Frequency System Mode at Liftoff Versus Pump Gain Product for Several Accumulator Volumes

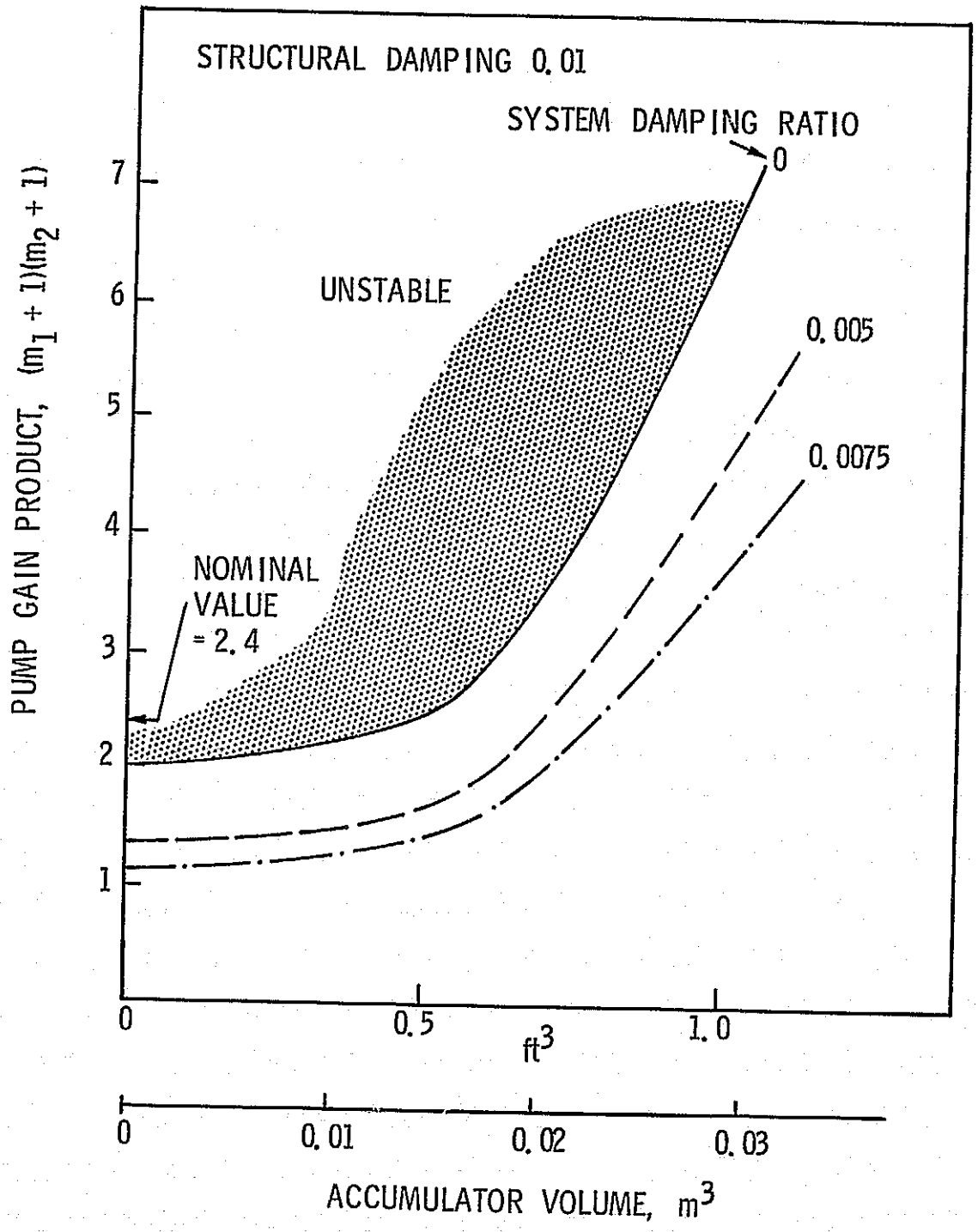

Figure 16. Damping of Low-Frequency System Mode at Liftoff Versus Pump Gain Product and Accumulator Volume

move to a higher accumulator volume. Thus, as in the previous section, we see that the degree of benefit achieved from increasing accumulator volume is very much dependent on the lower bound assumed for the low-frequency structural frequency.

1.4 ACCUMULATOR DESIGN RECOMMENDATIONS

Based upon the set of parametric analyses that had been run with the simplified system model, the following recommendations were developed for the design parameters of a helium-charged accumulator located at the HPOTP inlet.

a. The volume of the accumulator should be 0.028 m^3 (1 ft^3) or greater

b. The inertance of the accumulator should be maintained at or below 0.017 MN s^2/m^5 (0.001 $sec^2/in.^2$)

c. Provision should be made in the accumulator design for the possible future addition of resistance [a target design level for resistance is 8.4 MN s/m^5 (0.5 $sec/in.^2$)].

2. MULTIENGINE MODEL AND STABILITY ANALYSIS

The development of a multiengine pitch plane model with a comprehensive description of the feedline geometry was undertaken to enable a more refined analysis of the pogo problem. The model and the initial stability results generated with the improved representation of the system are described in this section of the report.

2.1 ANALYTICAL MODEL AND PROCEDURES

The analytical model again incorporates the elements of the propulsion system associated with the lox circuit, as was done for the single-engine model. The three SSME's are modeled as individual elements; however, since the analytical model treats symmetric motions in the pitch plane, the motion of the two lower engines were taken to be identical. The overall geometric arrangement of the model is shown in Figure 17. Both the feedline and interpump duct geometries are modeled in more detail than in the previous single-engine model (compare Figure 17 with Figure 2). As before, to assure a good description of the higher organ-pipe modes of the feedline, the fluid flow in the long feedline segment that was along the external tank (the element between points 2 and 3 in Figure 17) was represented by the exact solution to a one-dimensional continuous compressible flow. The fluid flow in the interpump ducts and the remaining feedline segments was described by a combination of incompressible flow segments and local compliances. The local compliances were located in the vicinity of the feedline corners, the inlets and outlets of the LPOTP's and the inlets of the HPOTP's. The employed compliance values were based upon the effective compressibility of the fluid. The resulting flow description was viewed as providing an adequate description of compressibility effects in these line elements for the frequency range of interest (frequencies below 30 Hz); in the single-engine model the interpump duct flows had been treated as incompressible and the lateral feedline (see Figure 2) was modeled for continuous compressible flow.

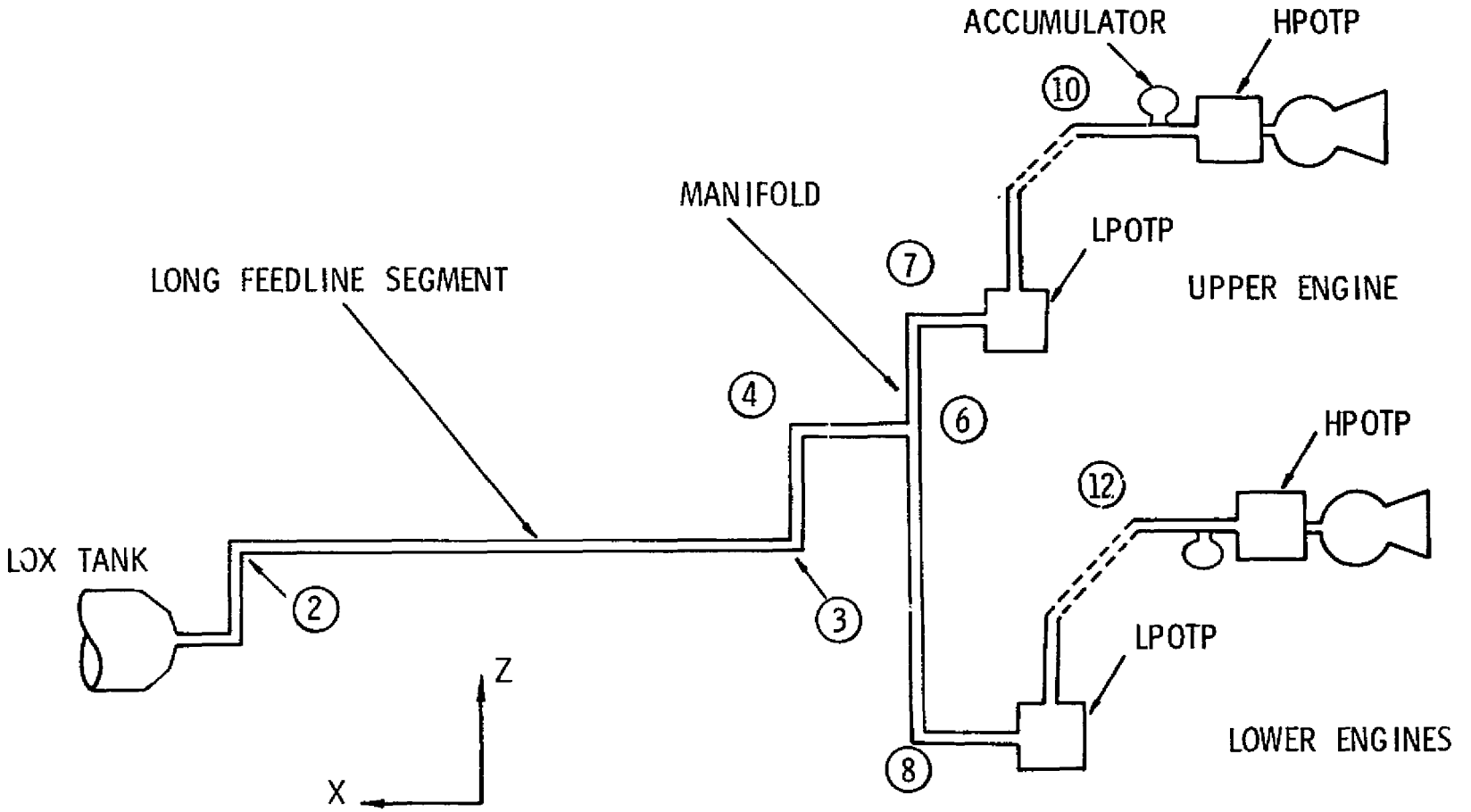

Figure 17. Schematic of Multiengine Model

In the stability analyses, the motion of the Shuttle vehicle was now represented by a series of up to ten pitch-plane structural modes, rather than by a single structural mode. The procedure used to determine the system stability was identical to that employed previously, namely, determination of the system eigenvalues and eigenvectors from the condition that the determinant of the system equations vanishes.

2.2 NUMERICAL INPUT DATA

2.2.1 Structural Mode Data

The structural mode data used in the analyses with the multi-engine model were provided by Rockwell International/Space Division. The data were associated with Shuttle model 4.3 and were of more recent origin than the data employed in the preceding parametric study and the studies of Refs. 3 and 4. The data comprised the frequencies and modal amplitudes of a selected set of pitch plane modes of vibration of the vehicle. The set has been selected by Rockwell upon the basis of the modal amplitudes of the elements of the system that were of concern in the pogo problem (i.e., engine gimbals, feedline corners, etc.). Data were supplied for seven flight conditions. In the assignment of the modal amplitudes, the corners immediately upstream of the LPOTP's and HPOTP's (points 7, 8, 10 and 12 in Figure 17) were assigned the same motion as the associated pump. The motion of the manifold and the longitudinal displacement of the corner immediately ahead of the manifold (points 6 and 4 in Figure 17) were generally assumed to be zero; this was done since the structural definition was not sufficiently adequate to define these modal motions. The assumption was not expected to be critical since the length of the feedline segment between points 4 and 6 was small compared to the length of the long feedline segment (the relative insensitivity was later confirmed by the study results). As before, to account for damping in the vehicle, a critical viscous damping ratio of 0.01 was assigned to each structural mode.

2.2.2 Propulsion System Parameters

The basis of the propulsion system parameters was identical to that employed in the preceding parametric analysis and the studies of Refs. 3 and 4. The variations of the nominal cavitation compliance values and pump gain values with flight time have been shown previously in Figures 3 and 4; the estimated and extreme values of these parameters for the liftoff, max q, after-SRB-separation, t = 254 sec and end-burn events are provided in Table 1.

2.3 STABILITY ANALYSIS

The stability of the system without pogo suppression is first examined for nominal conditions. A variety of parametric variations are then undertaken in order to examine the sensitivity of the system stability to various perturbations. The results obtained with the multiengine model are then compared with the results obtained previously with the single-engine model. Finally, the effect of an HPOTP inlet accumulator is examined.

2.3.1 Stability of System Without Suppression

2.3.1.1 Nominal Conditions

The multiengine system model was first employed to examine the stability of the system for nominal conditions. The analyses were run using the structural mode frequencies predicted by Rockwell and the nominal pump gain and cavitation compliance values employed by both Aerospace and Rockwell. Table 1 contains the Aerospace nominal values of the pump parameters; the nominal values employed by Rockwell are

$$C_{b1} = 0.39\ 10^{-3}\ m^5/MN\ (0.00667\ in.^2)$$

$$C_{b2} = 0.59\ 10^{-4}\ m^5/MN\ (0.001\ in.^2)$$

$$m_1 + 1 = m_2 + 1 = 1$$

The calculations were performed for five flight events: liftoff, max q, after SRB separation, t = 254 sec and end burn. Ten structural modes were employed per case; only nominal values were employed for the modal frequencies. The selected structural modes are listed in Table 2 together with the associated nominal frequencies. The minimum structural damping ratios that were calculated at each flight event for these nominal conditions are shown in Table 3; the structural modes associated with the minimum damping levels are also identified in the table. For illustrative purposes the predicted variation of the fundamental mode damping with flight time is also shown in Figure 18. From the presented results it is seen that stable conditions were predicted for every case that was treated. In fact any destabilizing influence of the propulsion system was generally minor, the worst case being the twenty-fifth mode at end burn (E25) where the damping ratio had been reduced from the assumed 0.010 level to a value of 0.0078.

2.3.1.2 Variation of Pump Parameters

As noted previously there is considerable uncertainty associated with the values of the inlet cavitation compliances and pump gains. To investigate the impact of variations in these parameters, stability analyses were run using the estimated maximum and minimum values of both the gain and compliance levels (see Table 1). The analyses were undertaken with ten modes at each flight event; the structural mode frequencies were fixed at their nominal values. The resulting minimum damping ratios calculated for these two pump parameter conditions are shown in Table 4; the particular mode associated with each minimum damping ratio is also identified in the table. Again, it is seen that stable conditions are predicted in all cases and that the destabilizing influence of the propulsion system is relatively minor; the worst case being the minimum damping ratio of 0.0062 that was predicted at the max q condition.

Table 2. Structural Modes and Frequencies in Nominal Case Analyses

Liftoff		Max Q		After SRB Separation		t = 254 sec		End Burn	
Mode	Freq. (Hz)	Mode	Freq. (Hz)	Mode	Freq. (Hz)	Mode	Freq. (Hz)	Mode	Freq. (Hz)
L1	1.97	Q1	2.26	A1	2.42	T1	2.54	E1	3.37
L2	2.35	Q15	9.15	A10	9.45	T8	9.40	E8	10.56
L3	2.46	Q20	11.09	A14	11.10	T10	11.05	E10	11.12
L20	11.09	Q40	19.15	A32	19.15	T11	11.09	E25	19.18
L44	19.2	Q41	19.22	A33	19.72	T29	19.05	E26	19.80
L52	22.26	Q48	21.90	A39	22.17	T36	22.25	E30	22.74
L53	22.88	Q49	22.81	A40	22.85	T37	22.88	E31	22.94
L64	26.55	Q58	26.55	A49	26.55	T45	26.55	E38	26.56
L72	28.88	Q67	28.89	A55	28.88	T51	28.88	E44	28.88
L99	40.0	Q93	40.0	A77	40.0	T73	40.01	E62	40.01

Table 3. Minimum Damping Ratios for Nominal Case Stability Analyses Without Accumulators; Nominal Structural Frequencies

Item / Event	Minimum Damping Ratio	
	Aerospace Nominal Pump Parameters	Rockwell Nominal Pump Parameters
Liftoff	0.0087 (L2)	0.0094 (L44)
Max Q	0.0092 (Q1)	0.0092 (Q40)
After SRB Separation	0.0092 (A55)	0.0094 (A32)
t = 254 sec	0.010 (T73)	0.0097 (T29)
End Burn	0.0078 (E25)	0.0090 (E25)

Table 4. Minimum Damping Ratios for Extreme Values of Pump Parameters Without Accumulators; Nominal Structural Frequencies

Item / Event	Minimum Damping Ratio	
	Aerospace Max Pump Compliance and Gain	Aerospace Min Pump Compliance and Gain
Liftoff	0.0073 (L52)	0.010 (L1)
Max Q	0.0062 (Q48)	0.010 (Q1)
After SRB Separation	0.0078 (A55)	0.010 (A1)
t = 254 sec	0.0079 (T51)	0.010 (T1)
End Burn	0.0087 (E44)	0.0098 (E30)

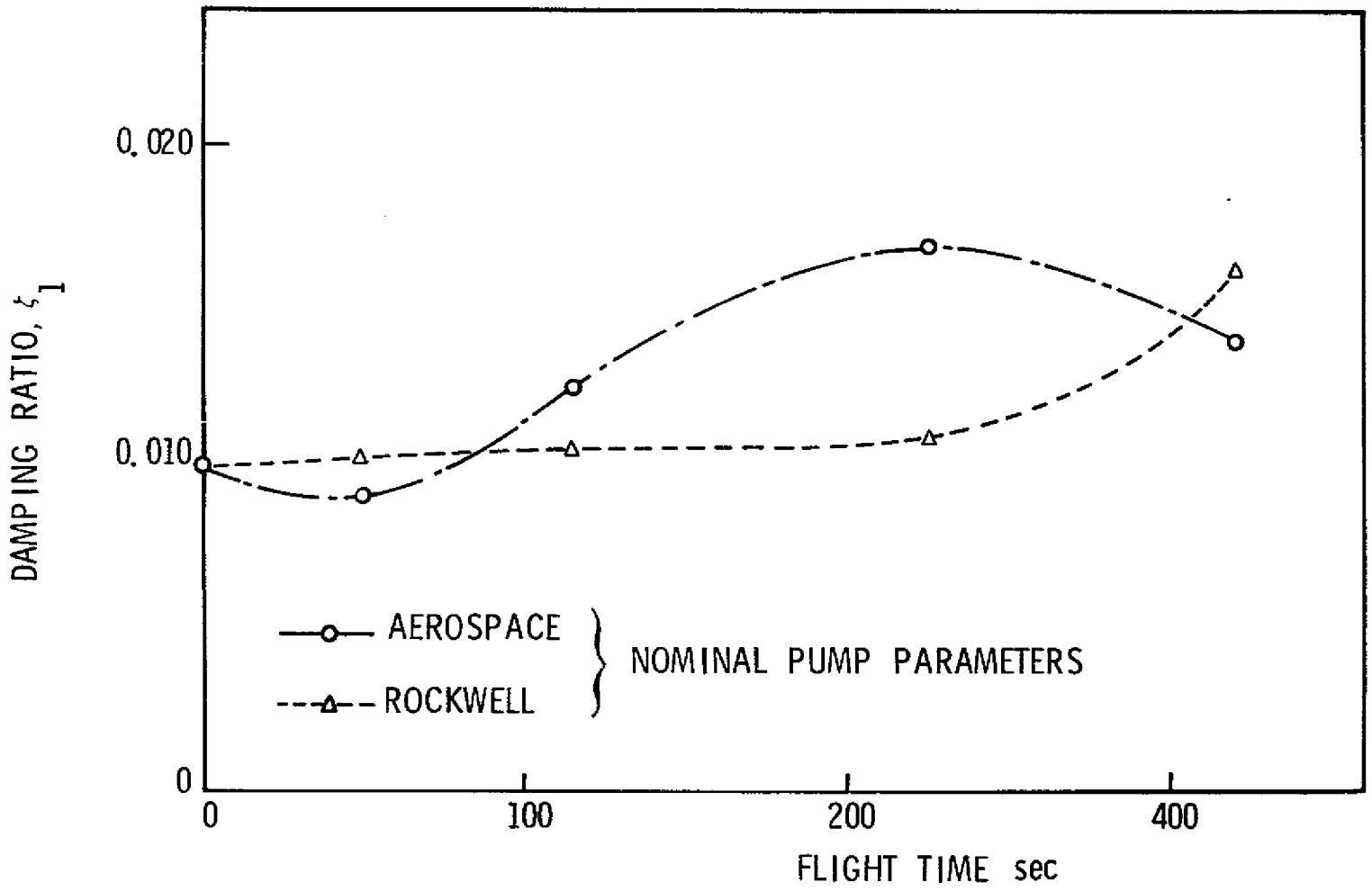

Figure 18. Variation of Low-Frequency Mode Damping with Flight Time for Nominal Conditions; No Accumulators

2.3.1.3 Variation of Structural Mode Frequency

The preceding results were obtained with the use of the nominal structural mode frequencies. Since the stability picture could change depending upon the relative proximity of the structural and propulsion system resonances it is important to determine the sensitivity of the system stability to variations in this proximity. In the earlier studies of Refs. 3 and 4 and the preceding parametric study (see Section 1 of the report), this sensitivity was examined by allowing each structural mode frequency to vary through a ±15 percent range about the nominal value. The same procedure was followed in the present analysis with the multiengine system model. The analyses were undertaken at liftoff, after-SRB-separation and end-burn events; the structural modes of interest were examined individually (i.e., single mode analyses were run for each mode over the ±15 percent frequency range). The resulting minimum damping ratios obtained with this procedure were 0.0078 for the L2 mode at liftoff, 0.0065 for the A55 mode at after-SRB-separation and 0.0089 for the E25 mode at the end-burn condition. The structural mode variations were then combined with the extreme variations in the pump gain. In this manner it was intended to represent a very severe condition for the system. The structural modes selected for this combined variation were the L2, L72, A55 and E25 modes. This selection was made upon the basis of the previous stability analyses. The resulting stability levels are illustrated in Figures 19 through 22 where the predicted damping ratios are presented as functions of the structural mode frequency for the maximum and minimum pump gain conditions; the results for nominal pump gain conditions are also shown in the figures for reference. Again it is seen that the system remains stable with the minimum damping ratios being maintained above a level of about 0.006. It will also be noted from Figures 20 and 21 that the minimum pump gain condition was more critical in the higher frequency L72 and A55 modes. A subsequent examination of the forces acting on these modes indicated that engine thrust was a stabilizing factor. Thus a reduction in pump gain (leading to a reduction in thrust) produces a reduction in the stability of these modes. This matter is discussed in more detail in Section 2.3.2.2.

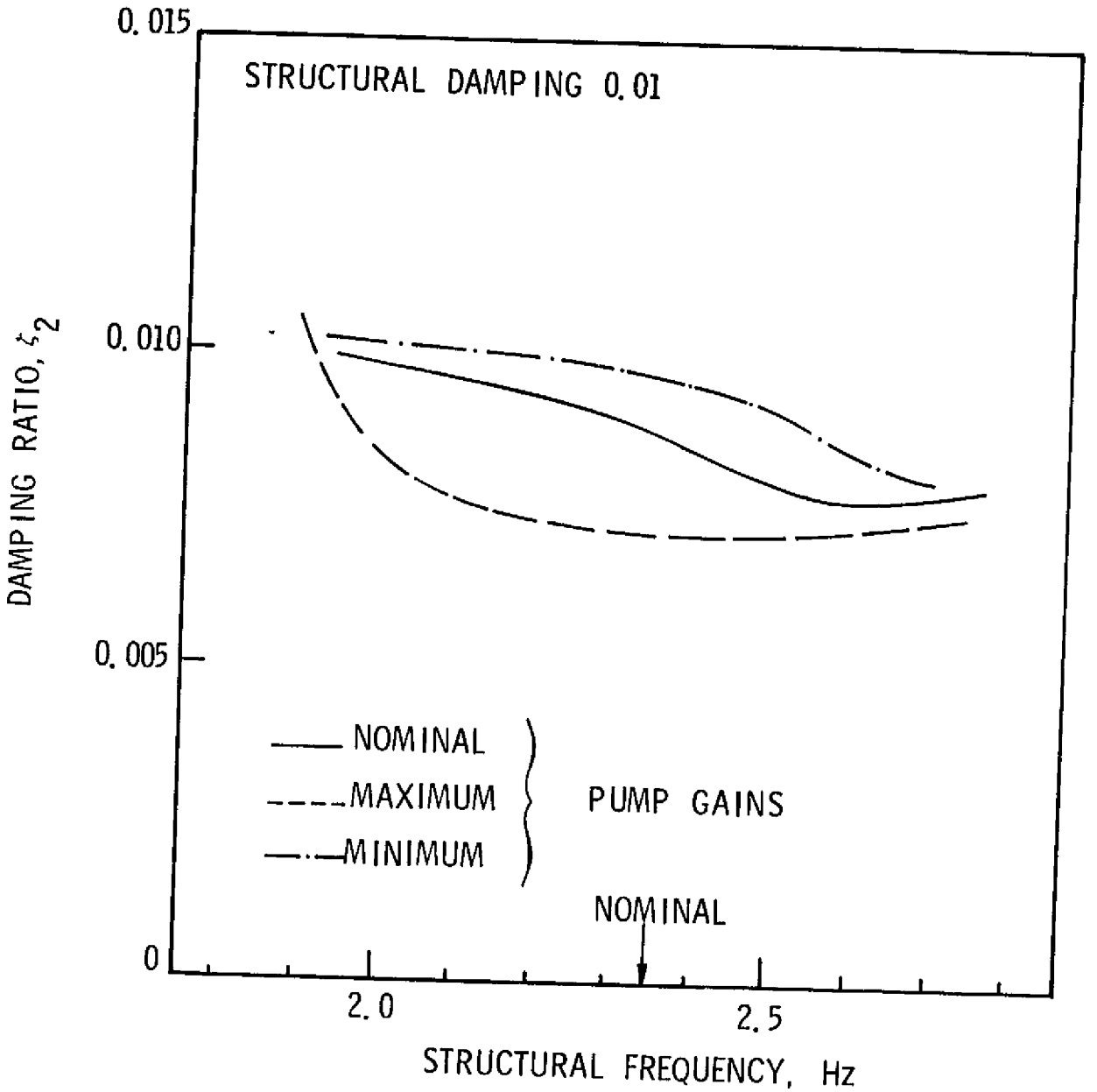

Figure 19. Stability Results as Function of Pump Gain: Low-Frequency Mode at Liftoff (L2); No Accumulators

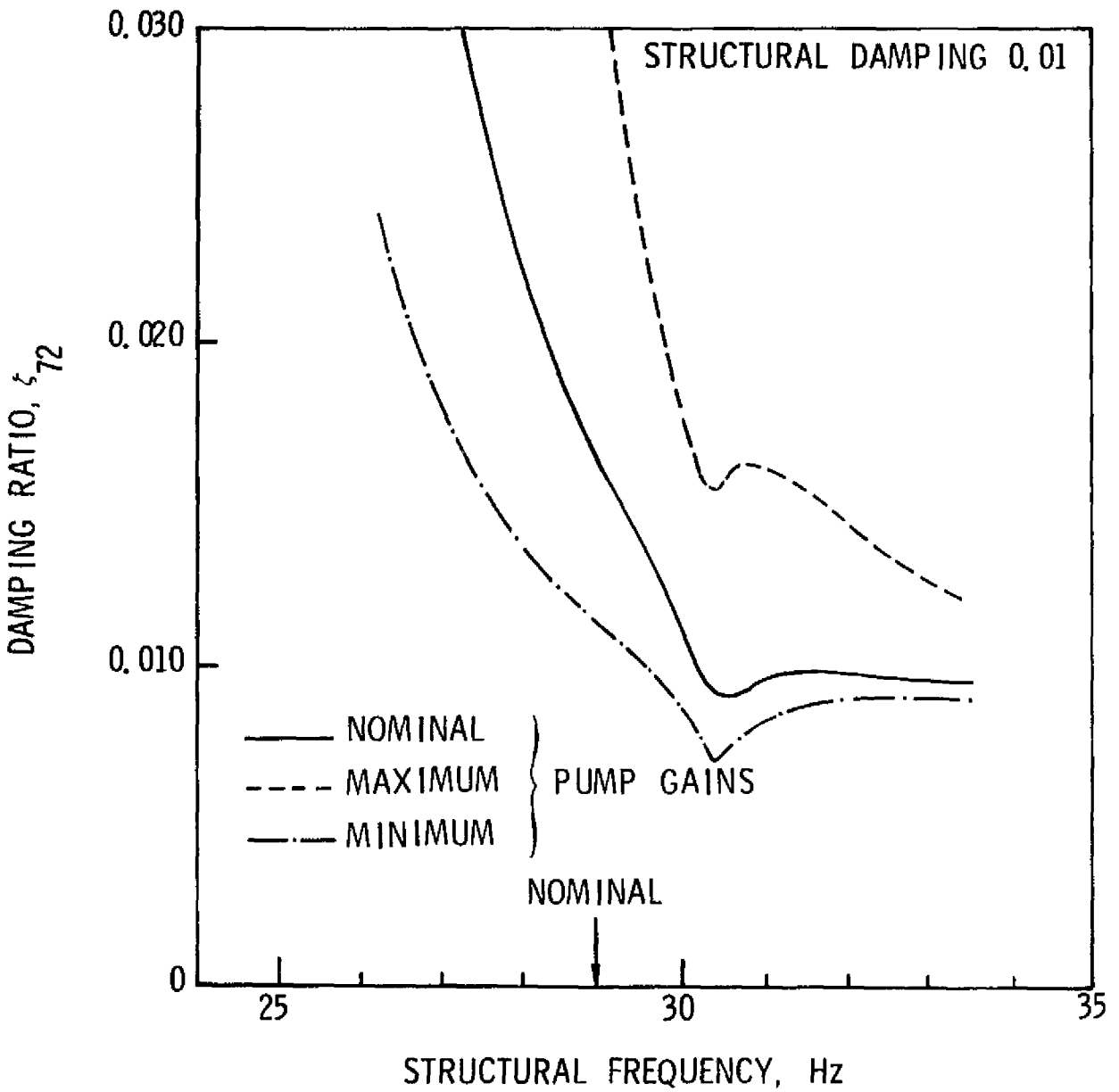

Figure 20. Stability Results as Function of Pump Gain: Liftoff Mode L72; No Accumulators

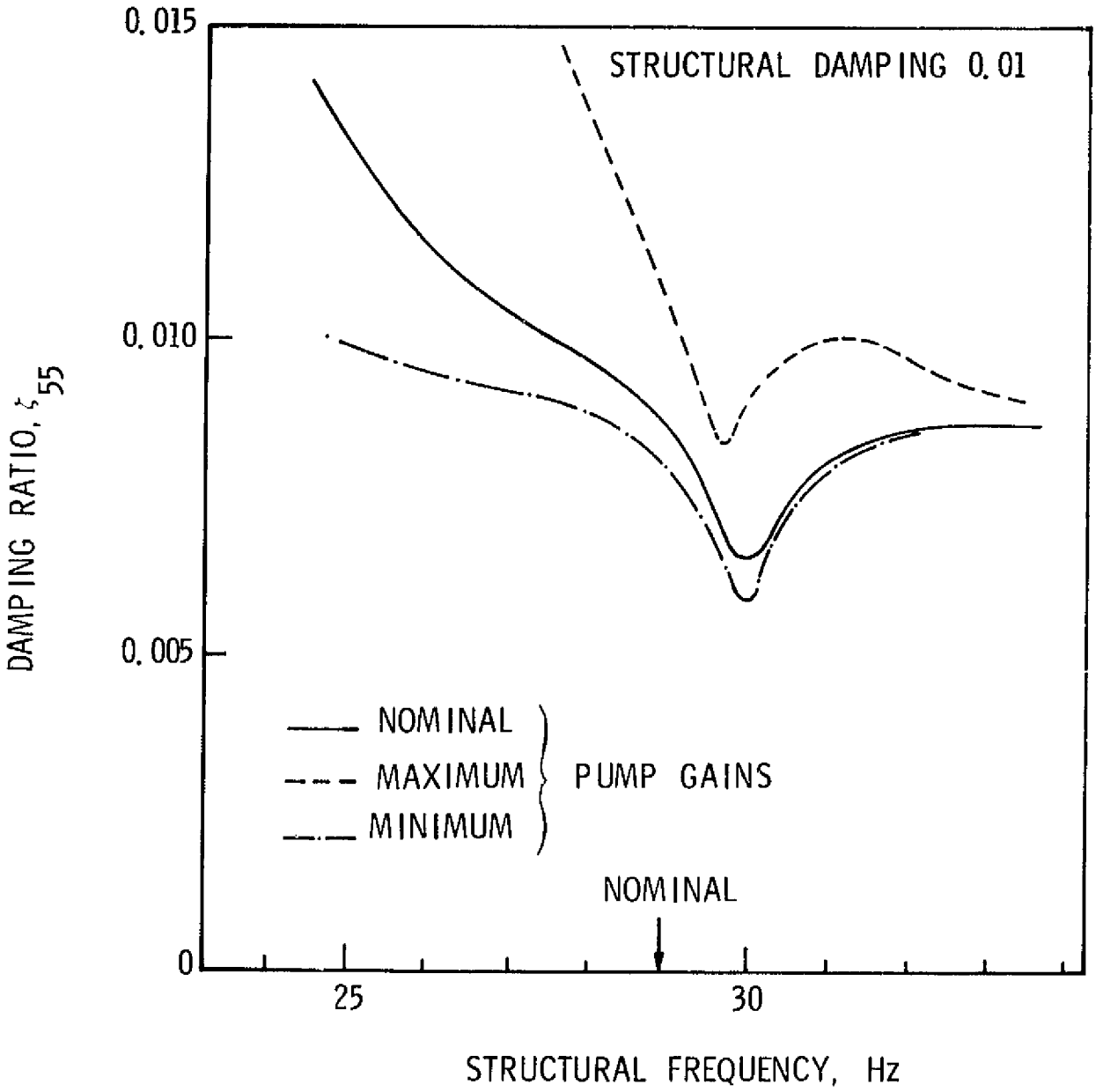

Figure 21. Stability Results as Function of Pump Gain: After-SRB-Separation Mode A55; No Accumulators

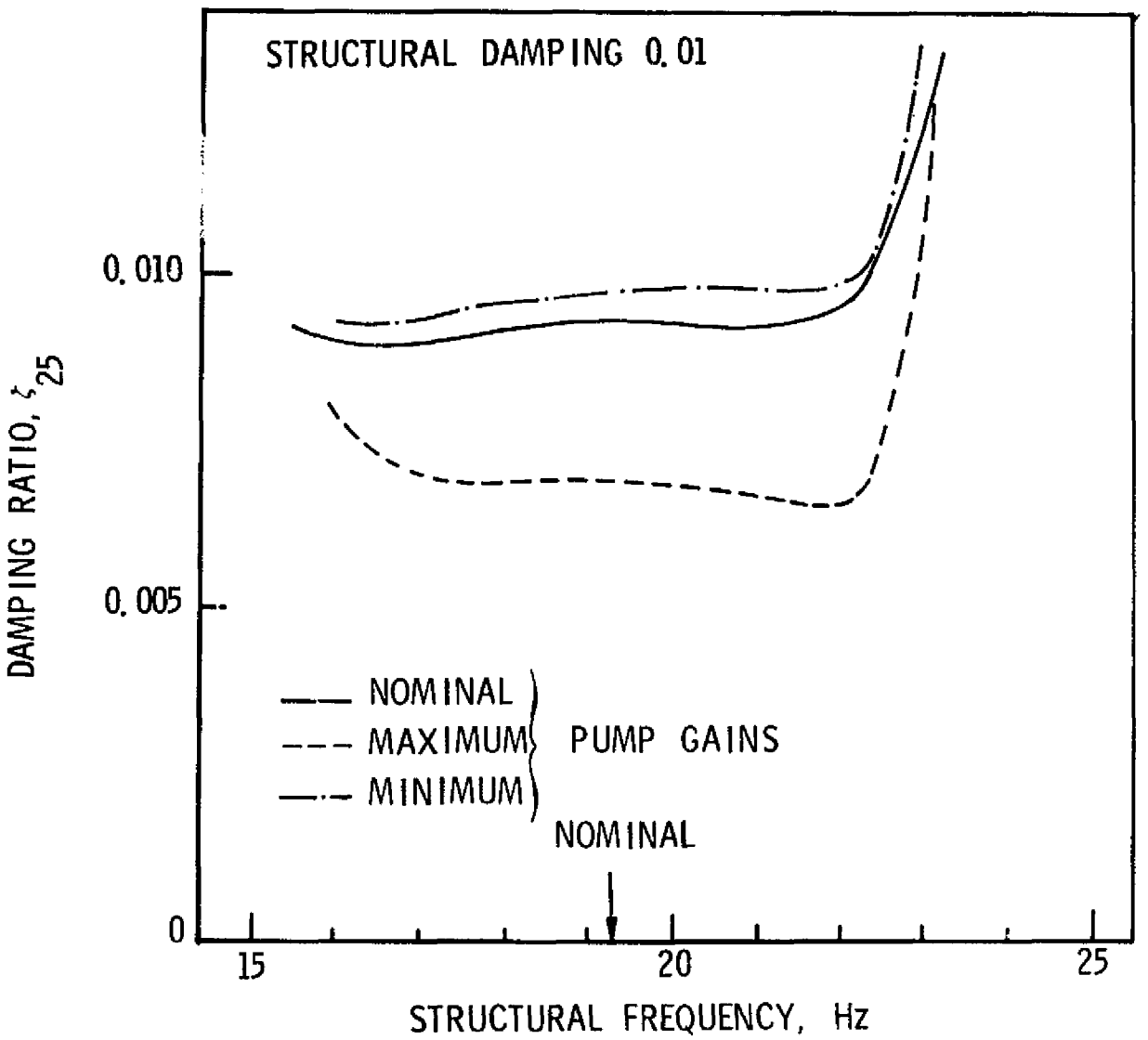

Figure 22. Stability Results as Function of Pump Gain: End-Burn Mode E25; No Accumulators

2.3.1.4 Variation of Structural Mode Shape

A limited examination was made of the sensitivity of the system stability to selected variations in the modal amplitudes. From an analysis of a simplified propulsion system (see Appendix A), it was found that perturbations in the engine thrust due to perturbations in the feedline motions were weighted by the length of the associated feedline element. Based upon this result, it was initially decided to run stability analyses with variations in the modal amplitude of the long feedline segment (called the "downcomer") that runs along the external tank (the element between 2 and 3 in Figure 17). The analyses were performed for the low-frequency modes at the liftoff, max dynamic pressure and after-SRB-separation events (i.e., the L1, Q1 and A1 modes, respectively) and for the second mode at liftoff (L2). The analyses were run using the ±15 percent variation about the nominal structural mode frequency. The results indicated a considerable sensitivity to variations in the selected modal amplitude. This sensitivity is illustrated in Figures 23 and 24 where the minimum damping ratios calculated for the L2 and A1 modes (over the assumed frequency range) are presented as functions of the ratio $\phi_x(3)/\phi_{xa}(g)$, where $\phi_x(3)$ is the longitudinal motion of the downcomer feedline segment and $\phi_{xa}(g)$ is the average longitudinal motion of the engine gimbals. Results are presented for the Aerospace nominal and maximum pump gain values and for the Rockwell pump gain of unity. The curves show dramatic losses in the stability of the system for the nominal and maximum pump gain conditions employed by Aerospace. It is seen that neutral stability is approached or an unstable condition developed by the time that the amplitude of the motion of the selected feedline segment has reached a level of some 30 to 40 percent of the average gimbal motion. In the supplied modal data the nominal amplitude of this feedline motion was less than 10 percent of the associated average engine gimbal motion (the data are provided at the downcomer support). Such levels lt from the presence of a node in the region of the feedline segment sup The adjustment of modal amplitudes in this region was considered to be prudent in view of the expected sensitivity of the nodal position to interface stiffnesses between the four Shuttle bodies and to payload dynamics.

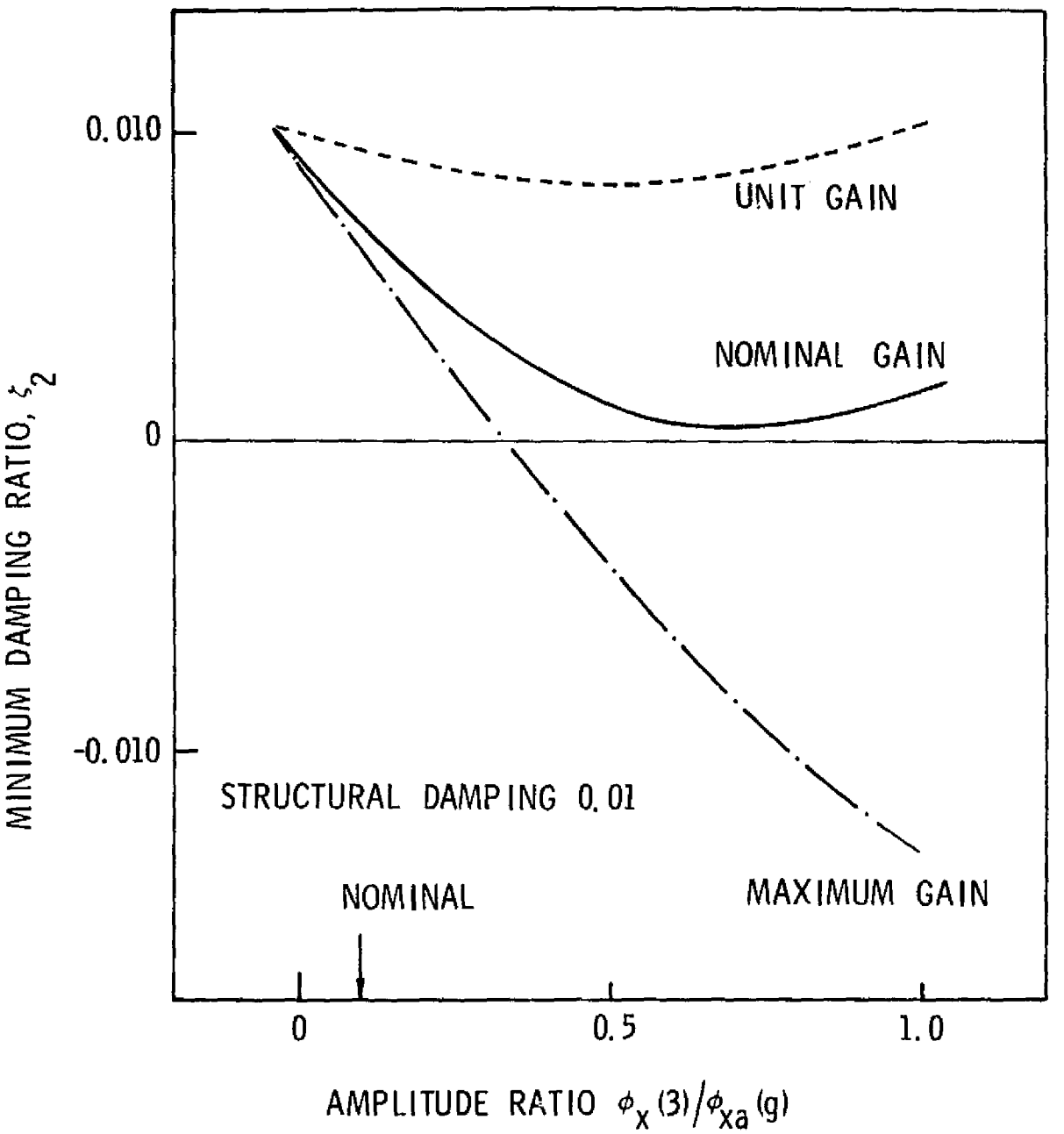

Figure 23. Damping Ratio Versus Downcomer Amplitude Ratio for Different Pump Gains; Low-Frequency Mode at Liftoff (L2); No Accumulators

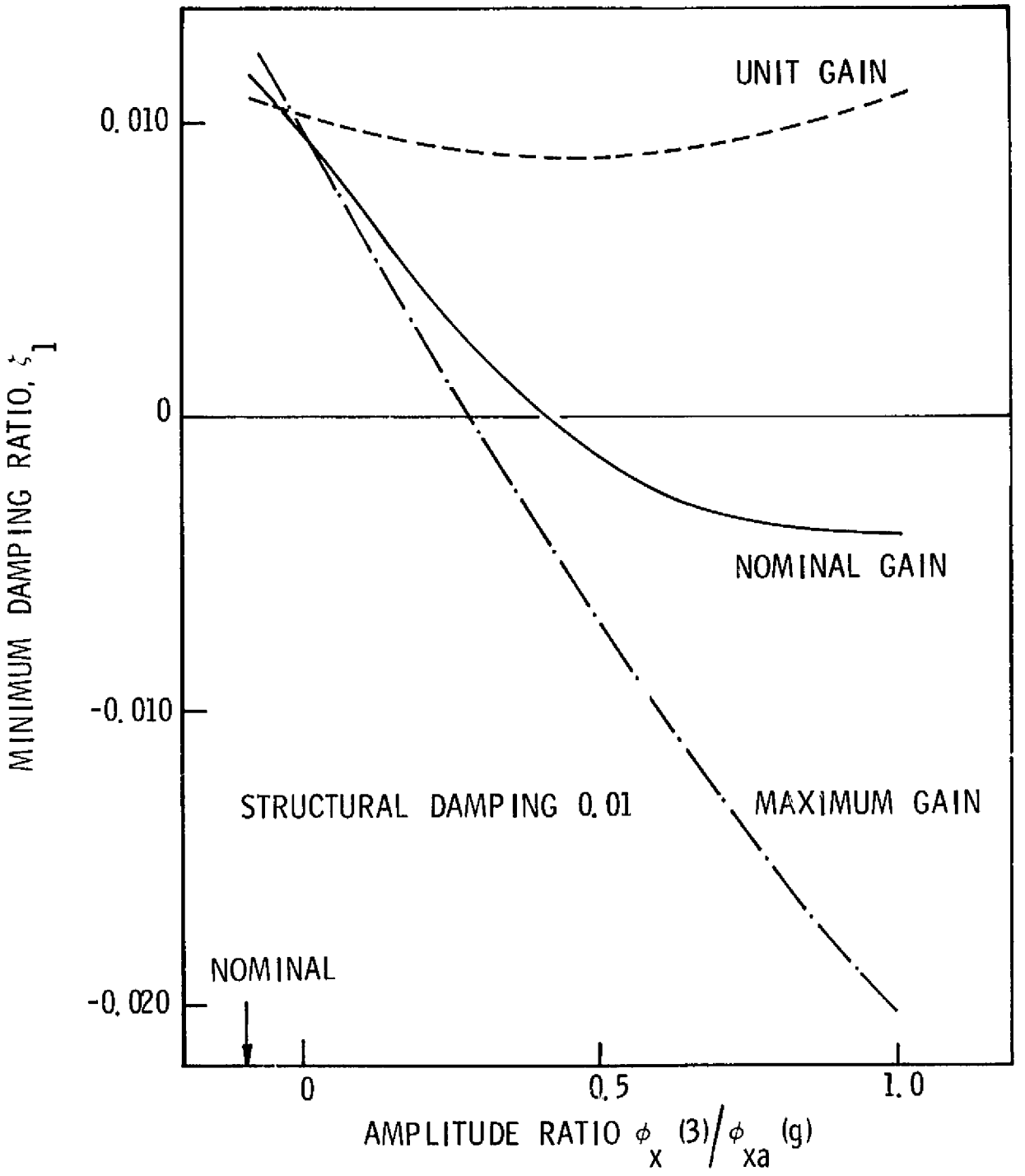

Figure 24. Damping Ratio Versus Downcomer Amplitude Ratio for Different Pump Gains; Low-Frequency Mode After SRB Separation (A1); No Accumulators

The effect of introducing longitudinal motion of the manifold and of the corner immediately ahead of the manifold (points 6 and 4 in Figure 17) was also examined. Stability analyses were run with the L2 mode using manifold and corner motions equal to the average motion of the LPOTP's; the resulting modal amplitude was some 4 percent higher than the average longitudinal motion of the engine gimbals. The predicted damping ratios shown in Figure 25 indicate that introduction of these motions does produce some degradation in the stability of the system; as anticipated, the degree of degradation is not as severe as that associated with the increased amplitudes of the feedline downcomer.

2.3.1.5 Comparison with Single-Engine Model Results

With the exception of the results obtained with the structural mode shape perturbation, specifically the long feedline downcomer aft support, the preceding analyses have indicated that the system remains stable over the selected variations in the input parameters. This behavior is at variance with the results obtained with the single-engine model where instabilities were found in both modes and a higher frequency mode (see Figures 5 and 6). Although the later analyses employed a more refined model and more current structural mode data, the variance was puzzling. This was particularly true for the case of the low-frequency mode behavior since the structural mode shapes had not changed dramatically. A detailed examination of this behavior indicated that the prime cause of the different qualitative behavior lay with the assignment of the modal amplitudes in the earlier model. In that model the amplitude of the motion of the corner immediately upstream of the low-pressure pump (point 3 in Figure 2) was different than the amplitude assigned to the low-pressure pump. Consequently a volume change was induced in the line element ahead of the pump. This change then served as a major de-stabilizing influence on the system. In the later model a more comprehensive description of the feedline geometry was provided and the assigned modal amplitudes were such that the introduction of such volume changes was

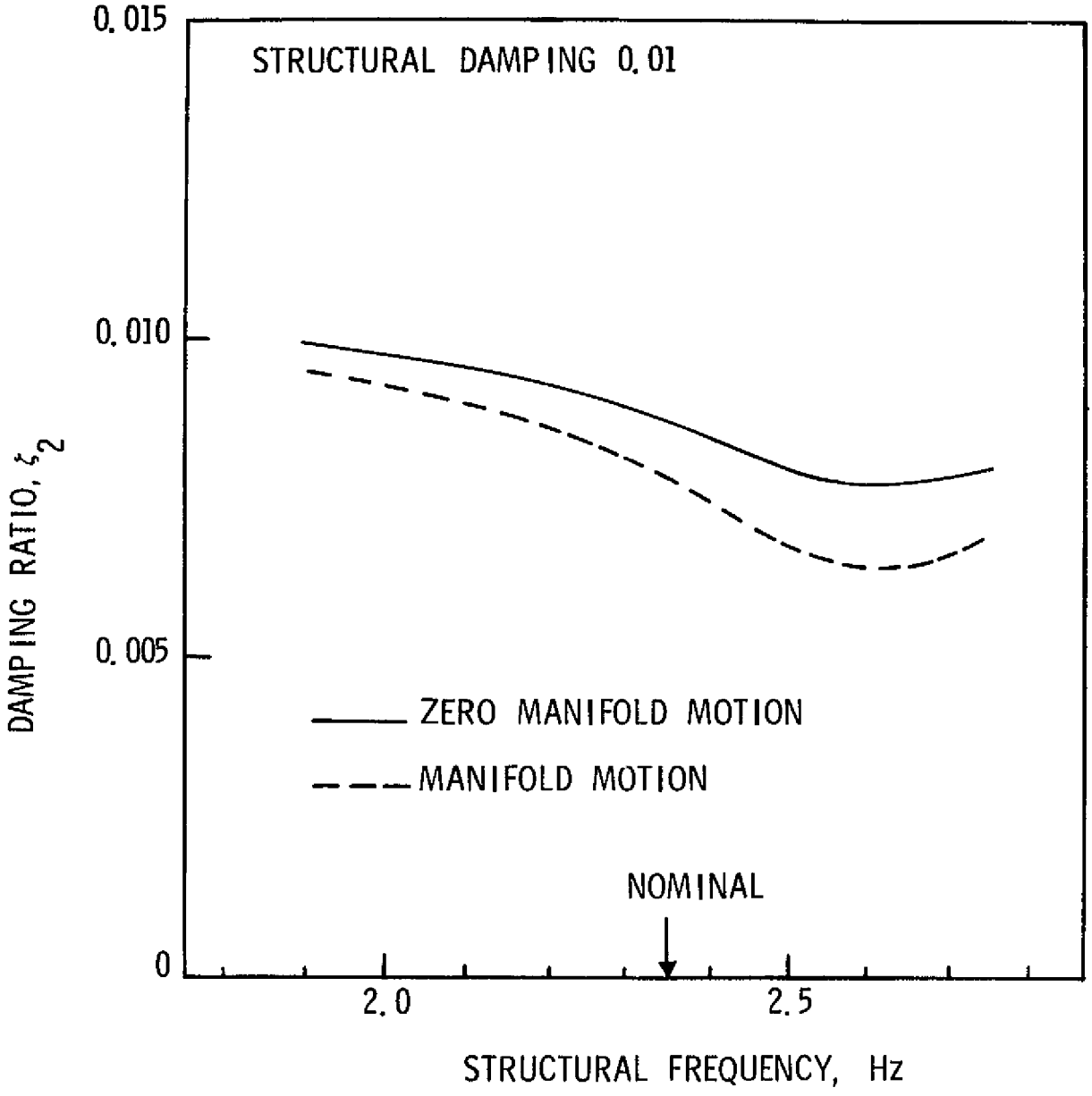

Figure 25. Effect of Manifold Motion on System Stability: Low-Frequency Mode at Liftoff (L2); No Accumulators

precluded. This preclusion of induced volume changes is consistent with the actual feedline design. Thus the later stability results are more representative of the system.

2.3.2 Stability of System with Accumulator

The effect of an accumulator upon the system stability for nominal conditions was first examined. The effect of varying the structural mode frequencies was next treated. Finally, the effectiveness of the accumulator in eliminating the instability that had been introduced by modification of the structural mode was examined. The bulk of these calculations was undertaken for a 0.017 m^3 (0.6 ft^3) helium-charged accumulator; this was the volume that had been selected for the baseline design on the basis of the prime contractor's (Rockwell International) recommendations.

2.3.2.1 Nominal Conditions

To investigate the effect of an accumulator upon the stability of the system a series of analyses was first run for nominal conditions. The accumulators employed in the analyses had volumes of 0.017 m^3 (0.6 ft^3) and were located two diameters ahead of the high-pressure oxidizer turbopumps. The analyses were performed for the flight conditions of liftoff, max dynamic pressure, after SRB separation, t = 254 sec and end burn. The resulting minimum damping ratios are shown in Table 5 together with the corresponding minimum damping ratios obtained for the system without accumulators; the structural modes associated with the quoted levels are also identified in the table. It is seen from the values given in the table that the changes in damping level due to the presence of the accumulators are minor.

2.3.2.2 Variation of Structural Mode Frequency

A limited examination was also made of the sensitivity of the damping levels to variation of the structural mode frequency. As previously, a ±15 percent variation about the nominal structural frequency was employed for this purpose. The results obtained for the low-frequency-liftoff mode (L2) are illustrated in Figure 26. It is seen that the presence of the accumulator

Table 5. Minimum Damping Ratios Calculated for Nominal Case Stability Analyses

Event \ Case	No Accumulator	0.017 m^3 (0.6 ft^3) Accumulator
Liftoff	0.0087 (L2)	0.0091 (L72)
Max Q	0.0091 (Q1)	0.0089 (Q67)
After SRB Separation	0.0092 (A55)	0.0082 (A55)
t = 254 sec	0.010 (T73)	0.0085 (T51)
End Burn	0.0078 (E25)	0.0075 (E31)

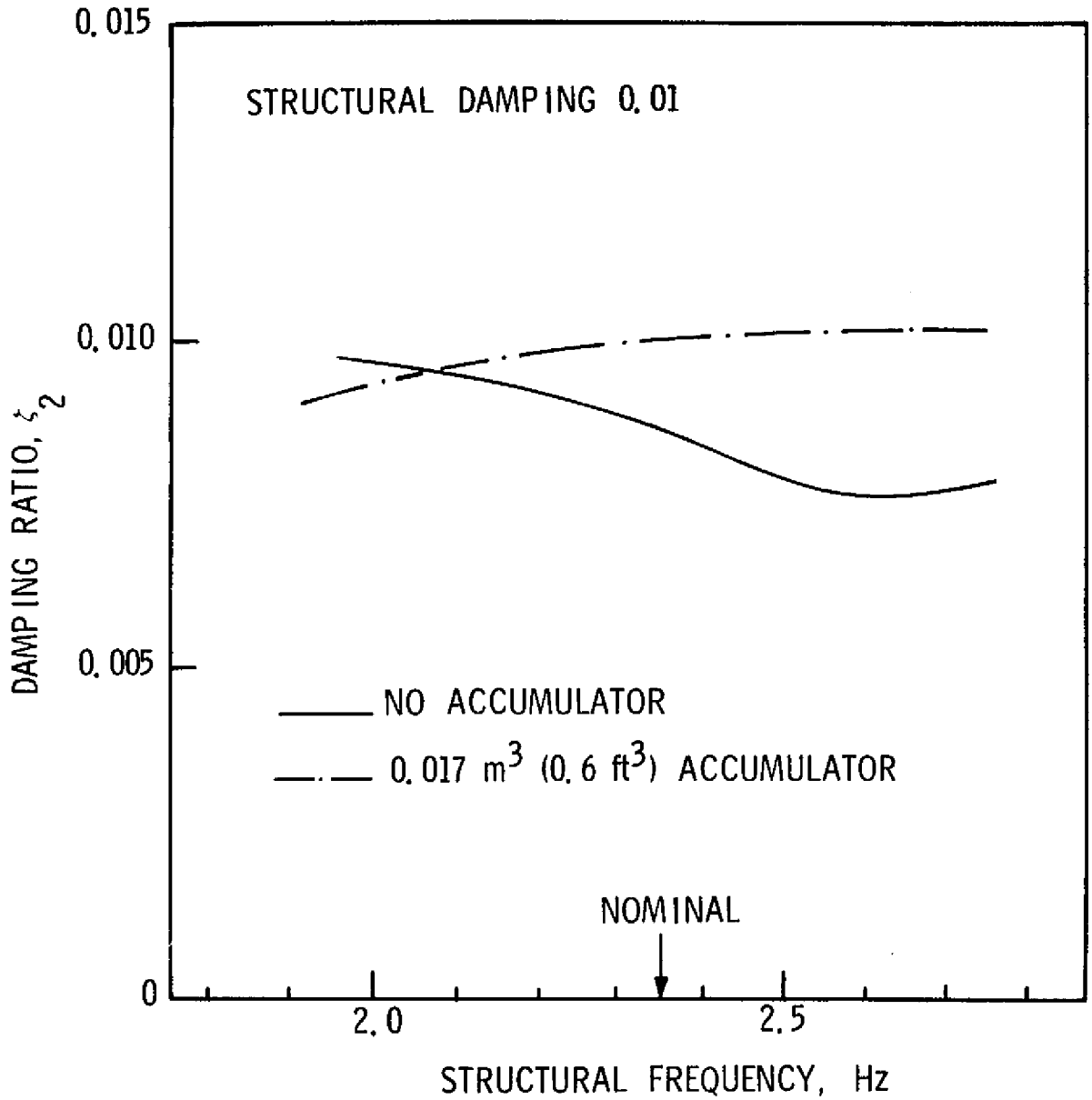

Figure 26. Effect of Accumulator on Lower Frequency Mode Stability: Low-Frequency Mode at Liftoff (L2)

enhances the stability of the mode at the higher end of the specified frequency range and slightly reduces the degree of stability at the lower end of the frequency range. The net result is an increase in the minimum damping level, associated with the assumed frequency variation, from a value of 0.0077 for the basis system to a level of about 0.009. The increase has been achieved by shifting the fundamental propulsion system mode frequency outside the ±15 percent tolerance band applied to the structural mode frequency (see Figure 14).

Results obtained for the higher frequency L72 mode are illustrated in Figure 27. In this case it is seen that the damping levels remain consistently below those associated with the no-accumulator system. This behavior was found to be due to the local nature of the structural mode (the predominant modal amplitudes are associated with the LPOTP on the upper engine). An examination of the energy transfer between the structure and the propulsion system indicated that the main destabilizing influence on the structural mode came from the forces acting on the LPOTP, whereas the thrust forces provided a stabilizing influence. The presence of an accumulator in this instance reduced the thrust forces and thus reduced the stabilizing influence of the thrust. The reduction in system damping in this case should not be taken to imply that the accumulator is potentially harmful. This is exemplified by the fact that when the structural damping in this L72 mode is reduced to zero and the system made passive (i.e., zero thrust and unit pump gain), the system does not become unstable, as shown in Figure 28. The interpretation of the behavior shown in Figure 27 is that the accumulator has simply changed the system mode shape such that a lower system damping results.

2.3.2.3 Variation of Structural Mode

In the analyses undertaken for the system it was found that instability could be introduced in the low-frequency modes by increasing the amplitude of the motion of the long feedline downcomer (see Figures 23 and 24). The effectiveness of the accumulators in eliminating such instabilities was examined. The amplitude $\phi_x(3)$ of the downcomer was taken to be

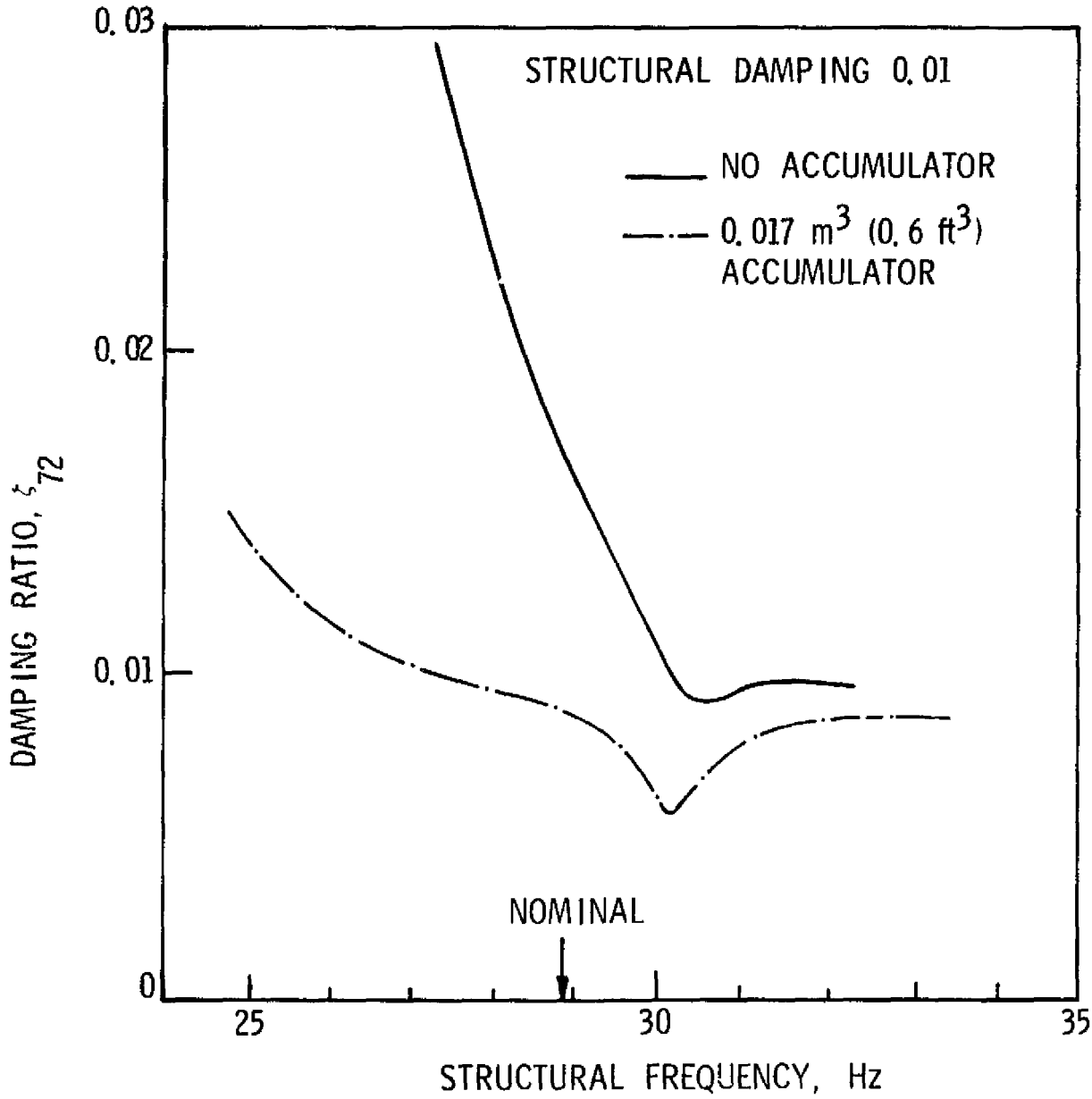

Figure 27. Effect of Accumulator on Higher Mode Stability: L72 Mode

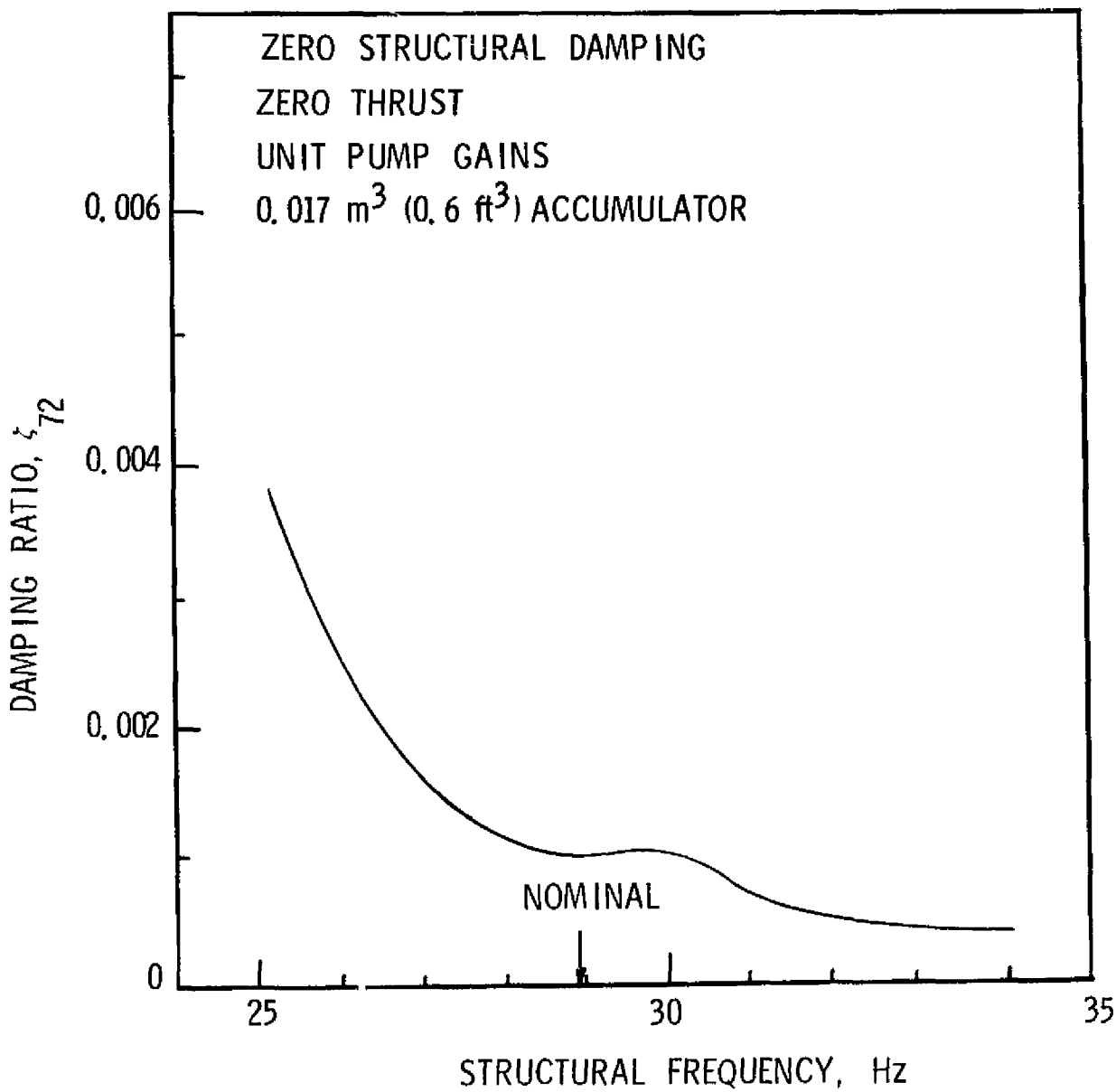

Figure 28. Stability Results for Passive System with Accumulator: L72 Mode

75 percent of the average engine gimbal motion and stability analyses were run for unit pump gain and Aerospace nominal and maximum values of pump gain. The resulting minimum damping ratios, over the ±15 percent frequency band, are illustrated in Figure 29 for the low-frequency mode after SRB separation (A1). Results are given for both 0.017 m^3 (0.6 ft^3) accumulator and 0.028 m^3 (1 ft^3) accumulator with the damping levels plotted against the pump gain product. The results clearly show the enhancement of the system stability produced by the presence of the accumulator with the greater improvement associated with the larger accumulator volume. The primary mechanism for such improvements is the shift of the propulsion system frequency away from the assumed frequency tolerance band associated with the structural mode frequency. This effect is illustrated in Figure 30 where the damping curves calculated for the A1 mode [with $\phi_x(3)$ equal to 75 percent of the average gimbal motion] and nominal pump gain are presented over the extended range of assumed structural mode frequencies for the no-accumulator case and for 0.017 m^3 (0.6 ft^3) and 0.028 m^3 (1 ft^3) accumulators. The ±15 percent tolerance band is shown in the figure together with the fundamental propulsion system mode frequencies for the three cases. It is seen that the minima in the damping curves appear in the vicinity of coincidence between the structural and propulsion system frequencies. Although the damping levels associated with these minima tend to improve with increase in the accumulator volume, it is seen that this improvement is minor compared to the effect produced by shifting the propulsion system frequency away from the ±15 percent tolerance band.

2.3.2.4 Imposed Phase Shift of Generalized Forces

Finally, the sensitivity of the system stability to imposed variations of the phase of the generalized forces acting on the structural mode was examined. This aspect of the system stability is of interest since the imposition of required phase margins is a possible element of the system stability requirements (Ref. 1). To examine this sensitivity, the stability of selected system modes was examined under conditions wherein the phase of every

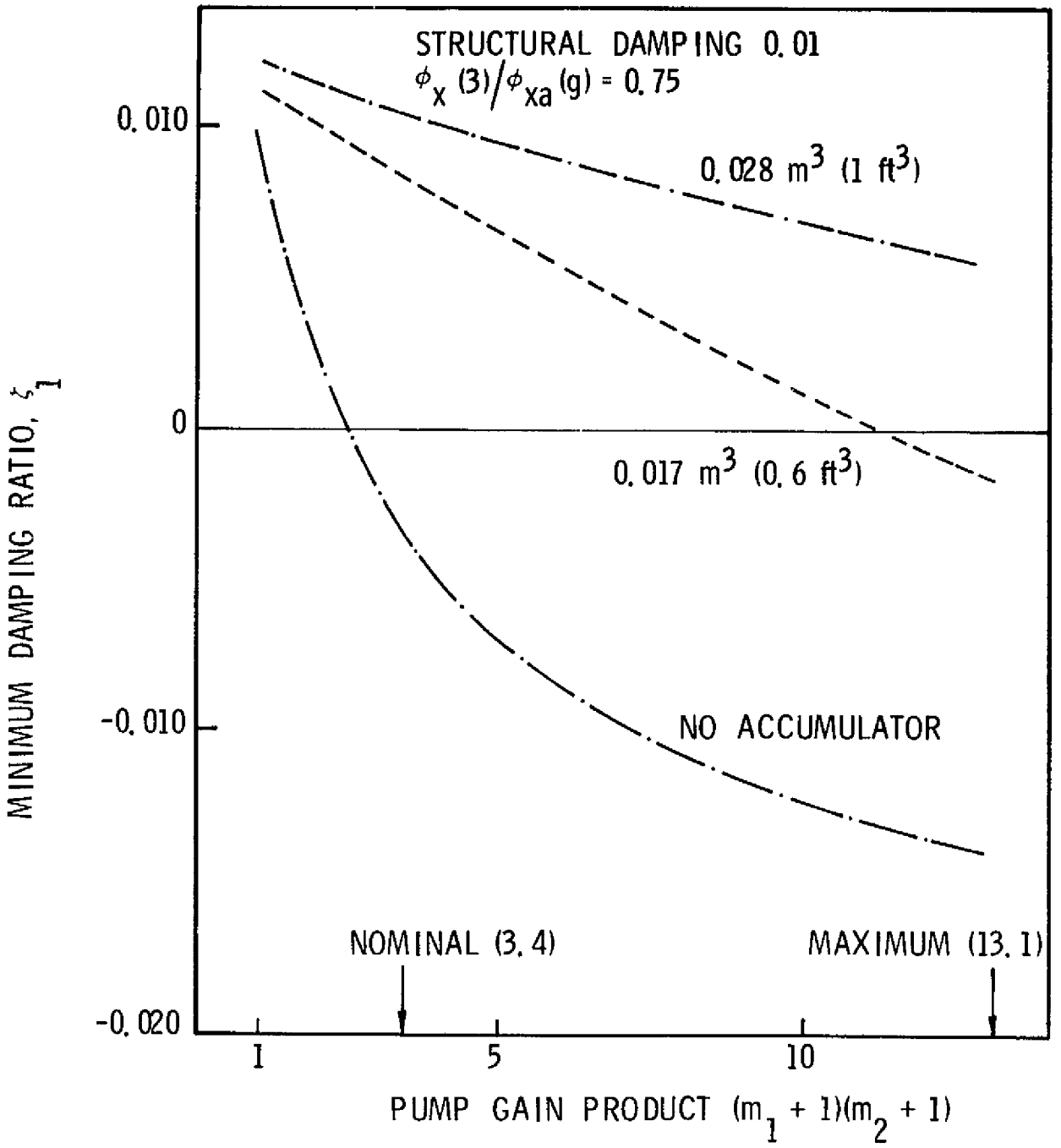

Figure 29. Damping Ratio Versus Pump Gain Product for Different Accumulator Volumes; A1 Mode, 0.75 Downcomer Amplitude Ratio

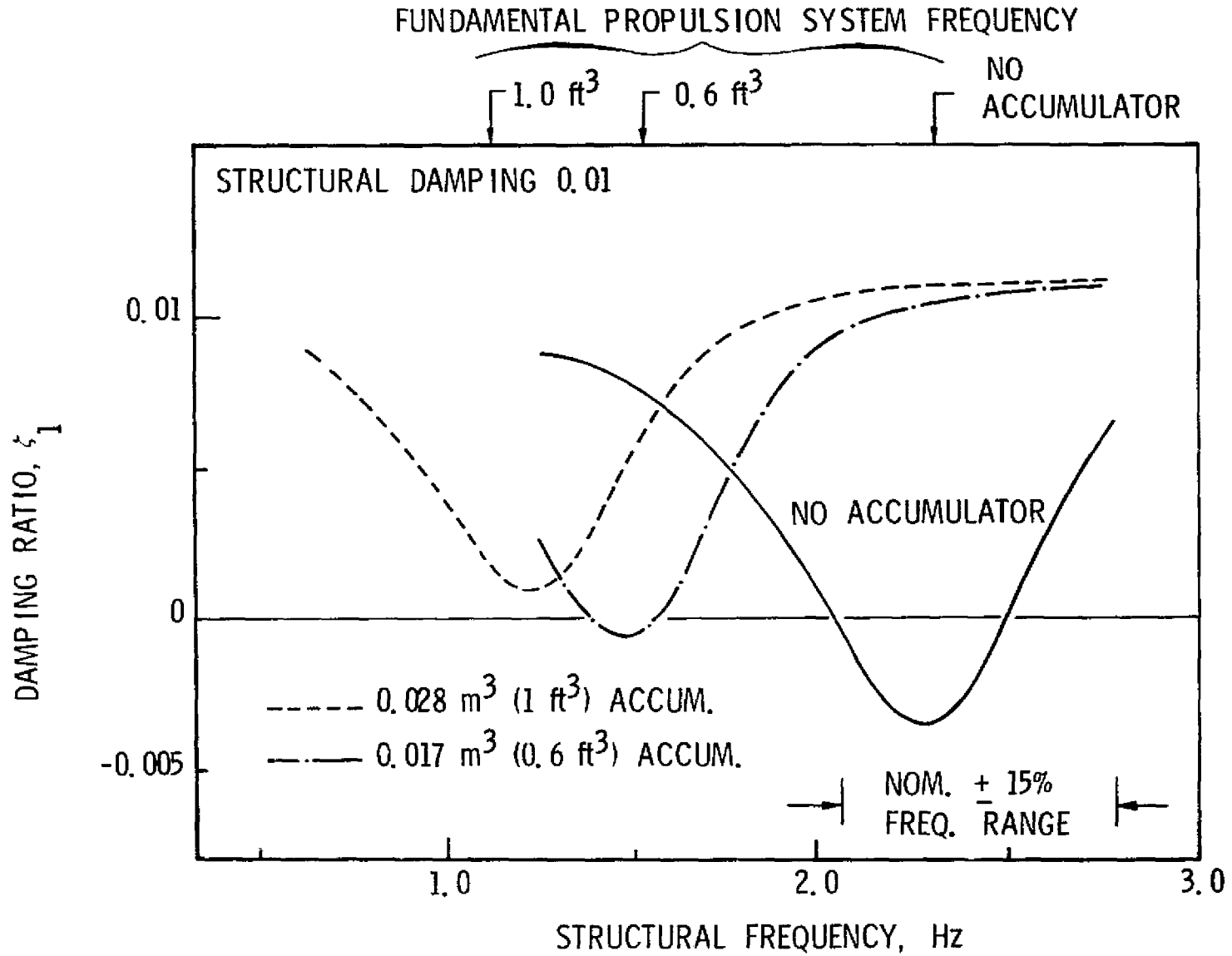

Figure 30. Variation of Accumulator Effectiveness with Structural Mode Frequency: A1 Mode, 0.75 Downcomer Amplitude Ratio

generalized force was arbitrarily changed by amounts of up to 45 degrees. The resulting stability boundaries indicated that the sensitivity to such variations was highly dependent upon the system mode in question. This feature is illustrated in Figure 31 where the minimum damping ratios, calculated over a ±15 percent range of the structural mode frequency, are plotted versus the imposed phase angle variation for the low-frequency liftoff mode (L2), the seventy-second liftoff mode (L72) and the low-frequency mode after SRB separation (A1). It is seen that the stability of the two low-frequency modes (i.e., the L2 and A1 cases) is relatively insensitive to the imposed variations in the phase shift of the forces, whereas the stability of the L72 mode is seen to be highly sensitive to the imposed changes in phase. The extreme difference in this sensitivity to phase change is due to the different character of the generalized forces that act on the system in the two cases. In the case of the L2 and A1 modes, the primary element in the overall generalized force is the thrust; at the minimum system damping condition the thrust forces are almost in phase with the generalized system velocity, consequently, the imposed changes in phase do not change the destabilizing influence dramatically. On the other hand, the primary destabilizing influences on the L72 mode are the forces acting upon the LPOTP in the upper engine; these forces are <u>almost</u> out of phase with the generalized velocity, consequently, the imposed phase shifts produce a significant change in the destabilizing influence on the system. It is of interest to see whether the sensitivity exhibited by the L72 mode could be removed by the presence of an accumulator. To investigate this question stability calculations were run with accumulators. The resulting minimum damping ratios are shown in Figure 32 for the system with a 0.017 m^3 (0.6 ft^3) accumulator. The presented results for this case still exhibit the same level of sensitivity as for the system without accumulators. The volume of the accumulator was subsequently increased arbitrarily to a value of about 0.23 m^3 (8 ft^3) and stability boundaries again developed. These boundaries proved to be essentially identical to the 0.017 m^3 (0.6 ft^3) accumulator results, thus showing that the sensitivity would not be

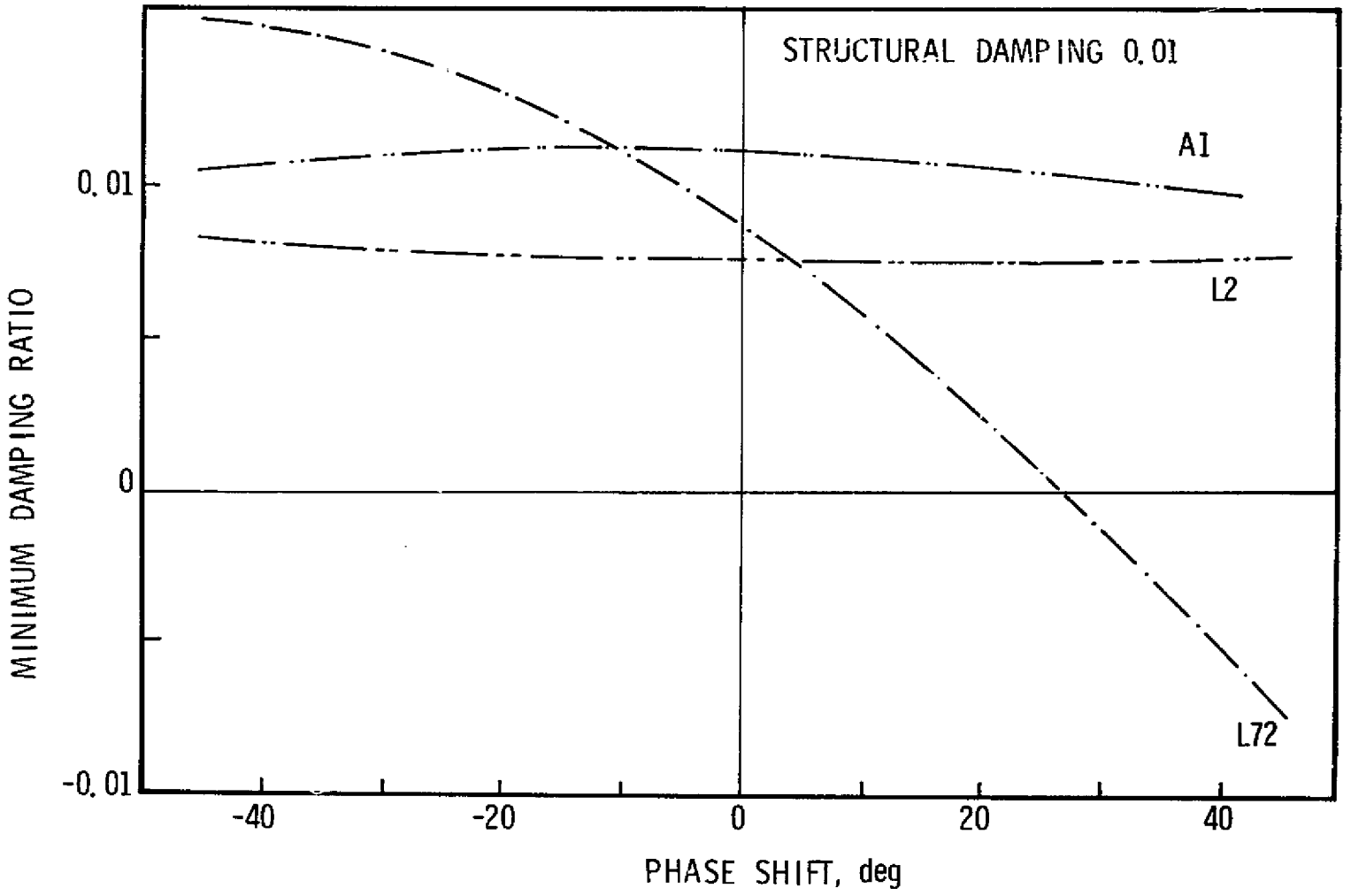

Figure 31. Stability Results for System Under Imposed Phase Shift on the Modal Generalized Forces; No Accumulators

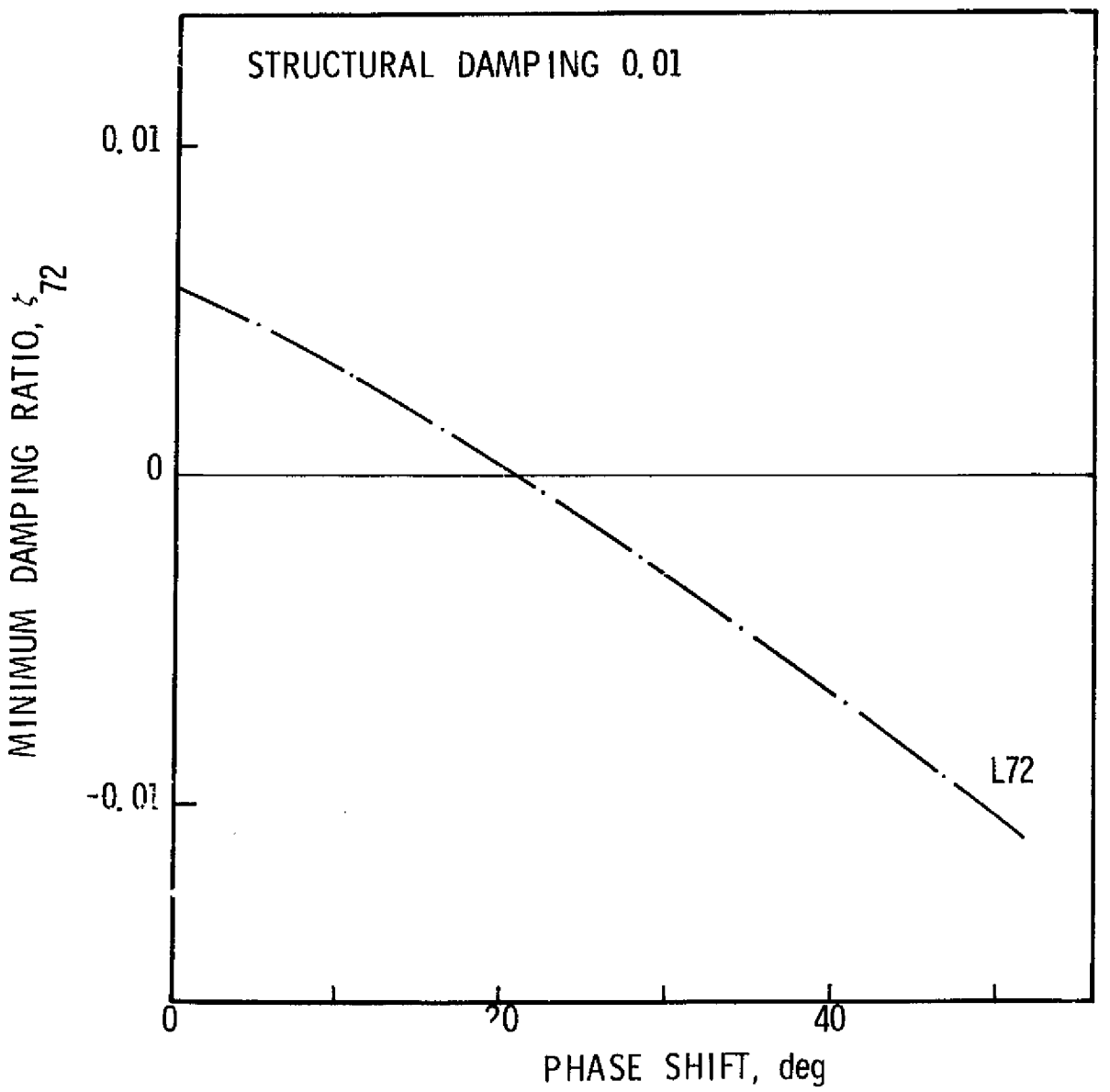

Figure 32. Stability Results for System with Accumulator Under Imposed Phase Shift on the Modal Generalized Forces: L72 Mode; 0.017 m^3 (0.6 ft^3) Accumulator

removed by the use of accumulators of reasonable size. Finally, the behavior of the L72 mode was examined in a purely passive system (i.e., unit pump gain, no thrust forces). The results (see Figure 33) indicated that the imposition of these phase changes causes the passive system to go unstable. The production of such an instability is completely unrealistic.

The net result of the above investigations is to show that the general use of a phase margin in the system stability requirements in the manner given in Ref. 1 is not appropriate. The reason for this is that the complexity of the Shuttle system can lead to situations in which forces that are not of direct active origin (i.e., non-thrust forces) can comprise the dominant component in the overall generalized force.

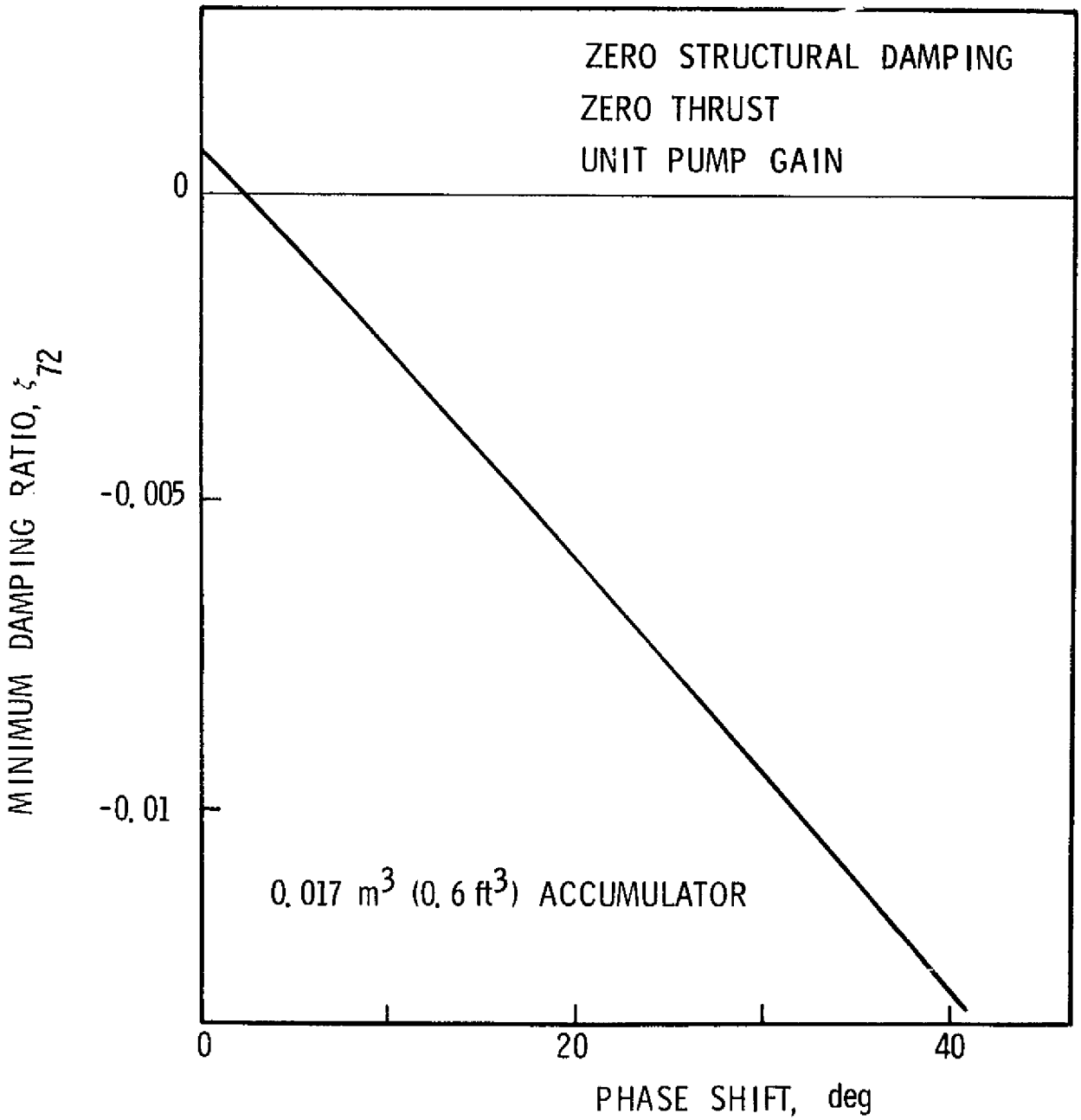

Figure 33. Stability Results for Passive System with Undamped Structure Under Imposed Phase Shift on the Modal Generalized Forces: L72 Mode with Unit Pump Gain, Zero Thrust, and Accumulator

3. SUMMARY AND CONCLUSIONS

An equivalent single-engine model was employed to develop the following set of design guidelines for the individual accumulators located at the HPOTP inlet:

a. A compliance corresponding to a helium volume $\geq 0.028\ m^3$ $(1\ ft^3)$

b. An inertance $\leq 0.017\ MN\ s^2/m^5$ $(0.001\ sec^2/in.^2)$

c. Capability for future incorporation of accumulator resistance of the order of $8.4\ MN\ s/m^5$ $(0.5\ sec/in.^2)$

The last guideline results from the possibility of instability due to coupling between the structure and the fluid mode associated with the fluid between the accumulator and the pump inlet. Accumulator resistance was shown to be highly effective in eliminating this type of instability.

An improved multiengine stability model has been developed; this model eliminates the inadvertent pumping which had been produced in the single-engine model and which is not possible in the actual system. The initial stability results obtained with the multiengine model have been described. These results indicate a generally stable system. The exceptional (unstable) case occurred when the amplitude of feedline downcomer longitudinal motion in the fundamental modes was increased from the values given in the provided modal data. These latter values were small, relative to the engine gimbal motion, due to the presence of a node in the area of the feedline downcomer support. Thus the adjustments of the modal amplitudes in this region were not considered to be excessive. The instability introduced in this manner was found to be eliminated by the addition of HPOTP inlet accumulators to the system. The results obtained with the refined model did not suggest a need to alter the design guidelines that had been developed with the single-engine model.

The multiengine model was also used to study the use of a phase margin in the system stability requirements. The results in this case indicated that use of a phase margin in the manner given in the NASA Space Vehicle Design Criteria (Ref. 1) is not appropriate.

APPENDIX A

ANALYSIS OF SIMPLE PROPULSION SYSTEM MODEL

It is assumed that

1. The feedline flows are incompressible
2. The feedline and pump have zero resistance
3. The pump gain is unity
4. The motion of the system elements is as shown in Figure A-1.

From the momentum and continuity equations for the system the pressure in the thrust chamber P_c can be expressed in the form

$$P_c = \frac{R_c}{Z}\left\{P_t + A\,Z_e\dot{X}_2 + As(L_1\dot{X}_1 - L_2\dot{Z}_1 + L_3\dot{X}_2)\right\}$$

where R_c denotes the resistance of the thrust chamber, A is the cross-sectional area of the feedline, Z_e is the engine impedance, s is the Laplace variable and the L_i denote the inertance associated with each of the three feedline segments. The quantity Z is defined by

$$Z = (L_1 + L_2 + L_3 + L_e)s + R_c$$

where L_e is the inertance of the engine. The velocities $\dot{X}_1$, $\dot{Z}_1$ and $\dot{X}_2$ that appear in the third term of the expression for P_c are the motions of the three individual feedline segments. These terms appear with coefficients that involve the product of the feedline area and the inertance of the associated feedline segment. These products are proportional to the length of the feedline segment. It is seen that the sensitivity of P_c, and thus the engine thrust, to these motions is weighted by the associated feedline length.

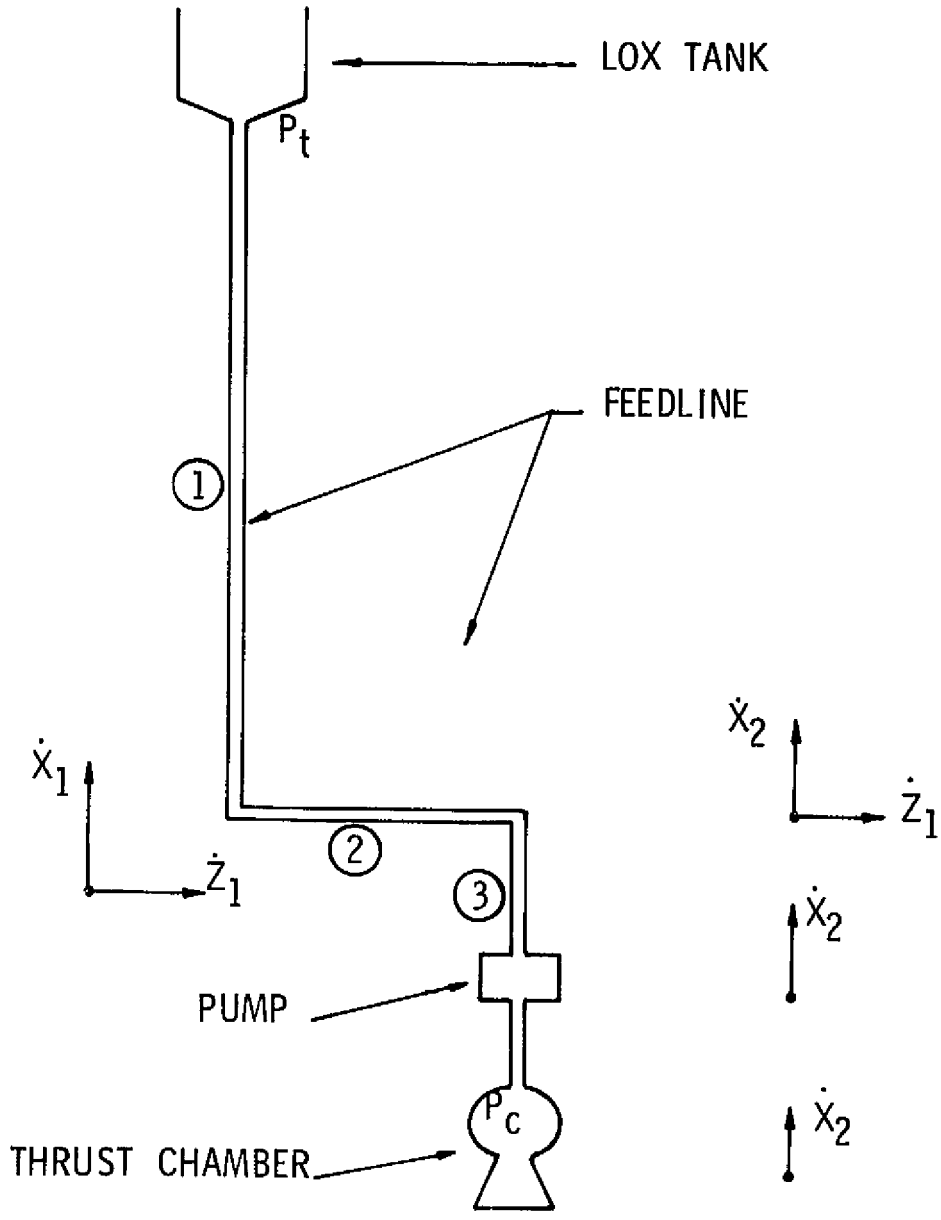

Figure A-1. Schematic of Simple Model

REFERENCES

1. Prevention of Coupled Structure-Propulsion Instability (Pogo), NASA Space Vehicle Design Criteria (Structures), NASA SP-8055, October 1970.

2. Rubin, S.; R. G. Wagner; J. G. Payne,: Pogo Suppression on Space Shuttle - Early Studies. NASA CR-2210, March 1973.

3. Lock, M. H. and S. Rubin,: Passive Suppression of Pogo on the Space Shuttle. NASA CR-132452, April 1974.

4. Lock, M. H. and Rubin, S.: Active Suppression of Pogo on the Space Shuttle. NASA CR-134749, October 1974.

5. Payne, J. G.; and S. Rubin,: Pogo Suppression on the Delta Vehicle. Report SAMSO-TR-74-187, The Aerospace Corporation, El Segundo, California, June 1974.

6. Holt, J. F.: ACS Mule, General Root Finding Subroutine. Report No. TOR-0073(9320)-8, The Aerospace Corporation, El Segundo, California, March 1973.

7. SSME Model, Engine Dynamic Characteristics Related to Pogo. Report No. RSS-8549-2, Rocketdyne Division, Rockwell International, Canoga Park, California, September 1973.

8. Ghahremani, F. G.; S. Rubin: Empirical Evaluation of Pump Inlet Compliance. Report No. ATR-73(7257)-1, The Aerospace Corporation, El Segundo, California, August 1972.